NASA/TM—2015-218816

Testing of Two-Speed Transmission Configurations For Use In Rotorcraft

David G. Lewicki and Mark A. Stevens
Glenn Research Center, Cleveland, Ohio

June 2015

NASA STI Program . . . in Profile

Since its founding, NASA has been dedicated to the advancement of aeronautics and space science. The NASA Scientific and Technical Information (STI) Program plays a key part in helping NASA maintain this important role.

The NASA STI Program operates under the auspices of the Agency Chief Information Officer. It collects, organizes, provides for archiving, and disseminates NASA's STI. The NASA STI Program provides access to the NASA Technical Report Server—Registered (NTRS Reg) and NASA Technical Report Server—Public (NTRS) thus providing one of the largest collections of aeronautical and space science STI in the world. Results are published in both non-NASA channels and by NASA in the NASA STI Report Series, which includes the following report types:

- TECHNICAL PUBLICATION. Reports of completed research or a major significant phase of research that present the results of NASA programs and include extensive data or theoretical analysis. Includes compilations of significant scientific and technical data and information deemed to be of continuing reference value. NASA counter-part of peer-reviewed formal professional papers, but has less stringent limitations on manuscript length and extent of graphic presentations.

- TECHNICAL MEMORANDUM. Scientific and technical findings that are preliminary or of specialized interest, e.g., "quick-release" reports, working papers, and bibliographies that contain minimal annotation. Does not contain extensive analysis.

- CONTRACTOR REPORT. Scientific and technical findings by NASA-sponsored contractors and grantees.

- CONFERENCE PUBLICATION. Collected papers from scientific and technical conferences, symposia, seminars, or other meetings sponsored or co-sponsored by NASA.

- SPECIAL PUBLICATION. Scientific, technical, or historical information from NASA programs, projects, and missions, often concerned with subjects having substantial public interest.

- TECHNICAL TRANSLATION. English-language translations of foreign scientific and technical material pertinent to NASA's mission.

For more information about the NASA STI program, see the following:

- Access the NASA STI program home page at http://www.sti.nasa.gov

- E-mail your question to help@sti.nasa.gov

- Fax your question to the NASA STI Information Desk at 757-864-6500

- Telephone the NASA STI Information Desk at 757-864-9658

- Write to:
  NASA STI Program
  Mail Stop 148
  NASA Langley Research Center
  Hampton, VA 23681-2199

NASA/TM—2015-218816

Testing of Two-Speed Transmission Configurations For Use In Rotorcraft

David G. Lewicki and Mark A. Stevens
Glenn Research Center, Cleveland, Ohio

National Aeronautics and
Space Administration

Glenn Research Center
Cleveland, Ohio 44135

June 2015

Level of Review: This material has been technically reviewed by technical management.

Available from

NASA STI Program
Mail Stop 148
NASA Langley Research Center
Hampton, VA 23681-2199

National Technical Information Service
5285 Port Royal Road
Springfield, VA 22161
703-605-6000

This report is available in electronic form at http://www.sti.nasa.gov/ and http://ntrs.nasa.gov/

Testing of Two-Speed Transmission Configurations For Use In Rotorcraft

David G. Lewicki and Mark A. Stevens
National Aeronautics and Space Administration
Glenn Research Center
Cleveland, Ohio 44135

Abstract

Large civil tiltrotors have been identified to replace regional airliners over medium ranges to alleviate next-generation air traffic. Variable rotor speed for these vehicles is required for efficient high-speed operation. Two-speed drive system research has been performed to support these advanced rotorcraft applications. Experimental tests were performed on two promising two-speed transmission configurations. The offset compound gear (OCG) transmission and the dual star/idler (DSI) planetary transmission were tested in the NASA Glenn Research Center variable-speed transmission test facility. Both configurations were inline devices with concentric input and output shafts and designed to provide 1:1 and 2:1 output speed reduction ratios. Both were designed for 200 hp and 15,000 rpm input speed and had a dry shift clutch configuration. Shift tests were performed on the transmissions at input speeds of 5,000, 8,000, 10,000, 12,500, and 15,000 rpm. Both the OCG and DSI configurations successfully perform speed shifts at full rated 15,000 rpm input speed. The transient shifting behavior of the OCG and DSI configurations were very similar. The shift clutch had more of an effect on shifting dynamics than the reduction gearing configuration itself since the same shift clutch was used in both configurations. For both OCG and DSI configurations, low-to-high speed shifts were limited in applied torque levels in order to prevent overloads on the transmission due to transient torque spikes. It is believed that the relative lack of appreciable slippage of the dry shifting clutch at operating conditions and pressure profiles tested was a major cause of the transient torque spikes. For the low-to-high speed shifts, the output speed ramp-up time slightly decreased and the peak out torque slightly increased as the clutch pressure ramp-down rate increased. This was caused by slightly less clutch slippage as the clutch pressure ramp-down rate increased.

Introduction

As part of the Revolutionary Vertical Lift Technology Project of the NASA Advanced Air Vehicles Program, research is being performed for large civil tiltrotors to replace regional airliners over medium ranges to alleviate next-generation air traffic. Aircraft design is to carry 90 passengers for 1,000 nm with performance of 300 knots at 28,000-ft altitude. Aircraft sizing-design studies have identified that a two-speed rotor configuration is required (Refs. 1 and 2). Rotor speed at cruise is required to be reduced, possibly down to 50 percent of hover speed, to keep rotor blade advancing tip speeds reasonable. To support this configuration, research in developing two-speed gearboxes is being led at the Glenn Research Center.

One early study of a multi-speed rotorcraft drive system consisted of a high-speed traction drive variator and a planetary differential gear unit (Ref. 3). A unit was tested and performed as designed. However, the mechanical efficiency was lower than that of a conventional drive system. Also, the use of traction drives for a main drive path is not an accepted practice for U.S. rotorcraft manufacturers. Previous studies have been sponsored by NASA to investigate multi-speed drive systems (Ref. 4). These

studies looked at earlier tiltrotor applications where 15 percent speed reduction for cruise was required. Dual-path configurations and compound planetary configurations looked promising. However, major concerns such as shifting and drive system weight were identified. An electro-mechanical, infinitely-variable transmission, comprising a pair of planetary trains interconnected with two electric machines and clutches, has been proposed (Ref. 5). Again, the mechanical efficiency suffered as well as the added complexity of two planetary systems. A unique concept called a pericyclic continuously variable-speed transmission is being investigated (Ref. 6). It uses pericyclic kinematics to achieve single-speed reduction ratios between 1.05:1 to 50:1 with variable-speed capability in one configuration. This concept, however, has yet to be tested.

An early example of clutches being employed in rotorcraft was in the XV-1 Convertiplane (Ref. 7). This aircraft was an autogyro with additional tip-jet propulsion on the rotors. When operating as an autogyro, a propeller was clutched-in to an internal combustion engine and de-clutched when flying in the tip-jet mode. In 1953, a two-speed helicopter transmission (Ref. 8) was flight tested on an Air Force H-5H helicopter. Here, engine speed was constant and main rotor speed was varied using a two-speed transmission. The flight tests showed that the two-speed transmission had great advantages in enhancing the rotorcraft performance. Another early example of the variable speed rotor concept was demonstrated with the XH-51 compound helicopter (Ref. 9). Here, rotor speed was varied by adjusting engine speed. In the flight tests, rotor speed was gradually decreased to reduce effects of advancing side tip speed compressibility effects resulting in lower vibrations, structural loads, and improved handling characteristics during high speed flight. Recently, a variable rotor speed approach was developed for the A160 Hummingbird unmanned aerial vehicle (Refs. 10 and 11). Here, a two-speed transmission is utilized to switch between two nominal rotor speeds. Then, rotor speed is continuously adjusted about either nominal speed through the engine power turbine set point.

Results from these previous references indicates that the incorporation of multi-speed concepts in rotorcraft application is not a trivial process and adds complexity and weight. Thus, further research and development in this area is required, such as described in (Refs. 12 and 13). There, studies were completed that investigated possible drive system arrangements that can accommodate up to 50 percent speed change. Several concepts where presented and evaluated. Two promising configurations were identified: 1) the offset compound gear transmission, and 2) the dual star/idler planetary transmission. These two configurations were designed and fabricated as part of the NASA Revolutionary Vertical Lift Technology Project. Further detailed information on the design of these configurations is given in (Ref. 14).

The objective of the current study is to present the results of the testing on the offset compound gear transmission and the dual star/idler planetary transmission. Testing was performed in the NASA Glenn Research Center variable-speed transmission test facility. Shift tests were performed on the transmissions up to the design speed of 15,000 rpm. Speed and torque transients as well as transmission component characteristics such as lubrication system parameters, vibration, and temperatures are presented.

Apparatus

Test Facility

Testing was performed in the NASA Glenn Research Center variable-speed transmission test facility. The variable-speed transmission test facility utilizes two identical alternating-current (AC) variable-speed motors which can be used as either a driver or a regenerative load. The facility implements a four quadrant, flux vector, high-performance drive system containing a common direct-current (DC) bus. The

common DC bus approach allows the power being absorbed from one motor to be utilized by the driving motor.

The test facility is shown in Figure 1. The two motors are custom-designed, 480-V, 3-phase, AC induction motors. The motors are water cooled using a dedicated cooling pump system. Each motor is supported internally by a pair of high-precision ball bearings, which are lubricated using an air-oil mist lubrication system. The motors also contain resistance temperature detectors (RTD's) on the motor windings and bearings, as well as a 1,024-tooth gear tachometer for speed control. The motors are rated for constant torque of 140 ft-lb from 0 to 7,500 rpm, and constant power of 200 hp from 7,500 to 15,000 rpm.

For the current studies, the left motor is the driver motor, providing the required input speed for the test. The right motor is the load device, providing open-loop torque, closed-loop torque, or closed-loop power control. The test transmission is installed between the two motors. The test transmission is configured with speed sensors and torquemeters on the input and output shafts. Due to the high speeds, the motors and transmission were installed using a high-precision laser alignment tool. The motors and test transmission incorporate jacking screws to aid in the alignment. High-speed couplings connect the components together.

The control scheme of the test facility is shown in Figure 2. The facility is powered by 480-V, 400-A AC service power which is isolated, filtered, converted to DC, and fed to the DC bus. The left motor is the driver and is configured for speed control. The left motor controller adjusts the speed of the motor based on the user set point using the motor tachometer for speed reference and its internal proportional-integral-derivative controller (PID) methodology. The right motor is the power absorber. For open-loop control, a fixed control is sent to the motor based on the user set point. For closed-loop control, information from the torquemeters is sent to the load programmable logic controller (PLC), which, in turn, sends the appropriate signal control to the motor based on the user set point. Under closed-loop torque control, the system tried to maintain a constant torque. Under closed-loop power control, the system tried to maintain constant power (speed times torque). Again, power absorbed by the right motor is fed back to the DC bus for use by the driver motor. Various analog, digital, and temperature measurements are fed to the data pod PLC. The left and right motor controllers, data pod PLC, load PLC, and control and data acquisition PC are all connected through an Ethernet hub. The control PC is the interface to the user, providing capabilities to adjust speed and torque, turn on lube system pumps, collect facility data, and monitor data for exceedance and shutdowns. Last, an emergency stop is available to immediately shutdown the facility if required.

The test transmission has a dedicated external oil lubrication system whose simplified schematic is shown in Figure 3. The system provides lubrication and cooling for the gears, bearings, and sprag clutch in the test transmission as well as providing high-pressure oil to the shift control clutch. Heated oil in the supply tank is pumped through a heat exchanger for precise temperature control. From there, the oil is split to the test transmission manifold and the high-pressure pump. The oil from the manifold is fed to jets that lubricate the gears and bearings in the test transmission as well as a feed to the sprag clutch in the test transmission. The oil from the high-pressure pump is fed to a servovalve that controls the shift clutch in the test transmission. Oil fed to the test transmission is returned to the return tank using a scavenge pump. For the tests, the oil was set to 160 °F oil inlet (to the test transmission) temperature and 80 psi oil inlet pressure. The lubricating fluid used was a synthetic base helicopter transmission oil conforming to the DOD-L-85734 specification.

Details of the shift clutch control system is shown in Figure 4. The purpose of this system is to provide the shift clutch piston with the proper pressure profile to achieve a required high-to-low or low-to-high speed shift. The high-pressure pump, as previously described, provides oil at 900 psi and 160 °F

temperature to the shift clutch servovalve. The servovalve is a flow control throttle valve and designed for precise pressure control with high dynamic response requirements. The output pressure of the servovalve, which is fed to the test transmission shift clutch piston, is set using a dedicated closed-loop, high-frequency, PID controller. User defined set points and pressure profiles are entered into the controller, which in turn, supply the required pressure to the shift clutch piston. The system can provide up to 800 psi pressure at 1 gpm flow rate.

Test Transmissions

Two different two-speed transmission configurations were tested in the current study. The first was the offset compound gear (OCG) transmission configuration. The second was the dual star-idler (DSI) planetary transmission configuration. Both are inline devices with concentric input and output shafts and designed to provide 1:1 and 2:1 output speed reduction ratios. Both are designed for 200 hp and 15,000 rpm input speed.

Transmissions used in rotorcraft applications are designed for light weight and minimized volume. The transmissions in the current study were designed, however, in a modular fashion. This was done to simplify modifications required when changing the design of various components in the test transmission such as the reduction gearing and shift clutch. In addition, a number of commercially available parts, many from the automotive industry, were used to reduce acquisition cost and fabrication time. Thus, the test transmissions in the current study were heavier and larger than actual rotorcraft counterparts, but were used to demonstrate prototype feasibility. The gearing, however, was designed using aerospace practices.

Offset Compound Gear (OCG) Transmission

A view of the OCG transmission is shown in Figure 5. As seen in the cross-sectional view (Figure 5(a)), the modular design is comprised of three regions: 1) the reduction gearing region, 2) the shift clutch region, and 3) the oil transfer region. The OCG employs a unique and patented arrangement in the reduction gearing region (Refs. 15 and 16). This is shown in a three-dimensional view in Figure 5(b). For this arrangement, the external OCG input gear, mounted on the input shaft, drives the internal OCG cluster gear 1. The external OCG cluster gear 2, integral with cluster gear 1, drives the internal OCG output gear. Note that the centerline of the cluster shaft is offset to that of the input and output shafts, thus giving the name “offset compound gear”. By using this unique arrangement of external and internal gearing, the envelope of the gearing is reduced compared to that using all external gears. Basic dimensions for the gearing are given in Table I. The OCG has a 2.005:1 reduction ratio and the output is driven in the same direction as the input. All gears were involute spur gears made from carburized and ground AISI 9310 alloy steel per AMS 6265M. The gears were made to high precision AGMA class 13. The input shaft, OCG cluster gear shaft, and output shaft were all supported by duplex ball bearing sets. All duplex bearings were installed in machined aluminum split cap and base supports which were mounted to the transmission housing steel base. The transmission housing itself was a square box structure made from aluminum plates, primary designed to contain the oil used in the transmission as well as ease of access to internal parts.

The two-speed OCG transmission operates as follows. The input shaft is directly connected to the forward side of the shift clutch. The aft side of the clutch is connected to the output shaft as in typical automotive applications. Under zero piston pressure, the clutch by default is mechanically engaged through spring force and the output shaft operates at the same speed of the input shaft. All the power flows directly from input shaft to output shaft at 1:1 reduction ratio. Here, the input shaft still turns the OCG input gear, OCG cluster, OCG output gear, and low-speed output drum (connected to the OCG output gear), but under no power. A sprag clutch is installed between the output shaft and low-speed

output drum and allows overrunning of the output shaft when its speed is greater than the output drum. To shift down in speed, pressure is applied to the shift clutch piston. When adequate pressure is applied, the clutch disengages and the output shaft coasts down in speed. When the output shaft speed reaches that of the low-speed output drum, the sprag clutch engages and the output shaft is driven at a 2.005:1 speed reduction through the OCG gearing. To shift back up in speed, the pressure to the shift clutch piston is released and the clutch is mechanically engaged, reverting back to the 1:1 ratio direct drive.

The shift clutch used in the studies was a commercially-available carbon clutch used in the automotive racing community. It is classified as a dry clutch and does not require oil for lubrication or cooling. A close-up of the clutch is shown in Figure 6. The clutch contains a pair of carbon-carbon plates. One of the plates is rigidly connected to the drive cover and the other is splined to the clutch inner shaft. Upon assembly, the plates are locked together as the clutch drive cover is bolted to the adapter shaft. This locks the input shaft (bolted to the adapter shaft) to the output shaft (bolted to the clutch inner shaft). To disengage the clutch, pressurized oil is applied to the piston, which pushes on the release fingers to separate the clutch plates. The bearings supporting the adapter shaft are sealed grease-packed deep-groove bearings which are axially preloaded by a Belleville washer spring pack located between the bearings. A grease-packed spider bearing is located between the input shaft and low-speed output drum. Dams and holes in the low-speed output drum were installed to keep the clutch area as dry as possible. Slight modifications were made from the original clutch design (described later) and the clutch capacity was approximately 150 ft-lb with a release load of approximately 425 lb, resulting in a required release oil pressure of approximately 325 psi.

As previously mentioned, oil was fed to the test transmission manifold to lubricate and cool the components in the transmission. Figure 7 shows details of the manifold as used for the OCG tests. Separate taps were used for the input shaft duplex bearing, output shaft duplex bearing, OCG cluster shaft duplex bearing, sprag clutch, and front and rear manifolds located in the test transmission housing. All taps had throttle valves to regulate oil flow rate. For the OCG tests, the front manifold fed the OCG input gear mesh into-mesh jet and OCG output gear mesh out-of-mesh jet. The rear manifold fed the OCG input gear mesh out-of-mesh jet and OCG input gear mesh into-mesh jet. Per trial and error, all throttle valves were set wide open except for the sprag clutch, which was throttled slightly closed. The approximate oil flow rates to the various OCG components as indirectly measured is given in Table II.

Lastly, Figure 5(a) shows the oil transfer region toward the aft side of the transmission. This region contains the oil transfer mechanism to supply oil to the rotating shift and sprag clutches. This was quite a design challenge due to the sealing requirements at these high speeds and high pressures. The oil transfer mechanics along with the custom designed output shaft supplied oil to three separate passages: 1) high-pressure oil supply to shift clutch piston, 2) high-pressure oil return bleed from shift clutch piston, and 3) low-pressure oil supply to sprag clutch. The oil in the passages were sealed in the oil transfer mechanism through use of Vespel polyimide (DuPont) sealing rings.

Dual Star-Idler (DSI) Planetary Transmission

The second transmission tested was the DSI planetary transmission as shown in Figure 8. This configuration is identical to the OCG except the OCG half-speed gearing was replaced with the DSI planetary configuration. As seen in the front view (Figure 8(b)), the DSI planetary has an input sun gear which drives three sets of star and idler planet gears, which drive an internal ring gear as the output. The planetary carrier is fixed to ground. The idler gears are needed to permit the ring gear to rotate in the same direction as the sun gear. All planet gears were straddle mounted with pairs of high-precision, high-speed, axially-preloaded duplex ball bearings. Basic dimensions for the gearing are given in Table III. The DSI

has a 2.020:1 reduction ratio. All gears were involute spur gears made from carburized and ground AISI 9310 alloy steel per AMS 6265M. The gears were made to high precision AGMA class 13.

The DSI configuration used the same shift clutch as the OCG tests. Thus, the operation of the shifting was identical to that of the OCG. Regions 2 and 3 for the DSI were identical to that of the OCG with one exception. A sprag clutch aft bearing was added to provide additional support to the low-speed output shaft drum. Lubrication to the DSI was slightly different than the OCG. The same manifold of Figure 7 was used but the OCG cluster duplex bearing tap was closed. The front manifold fed all 1 DSI planet bearings. The rear manifold fed all the DSI gearing using nine total jets, three per planet pairs. As with the OCG, all throttle valves were set wide open except for the sprag clutch, which was throttled slightly closed. The approximate oil flow rates to the various DSI components as indirectly measured is given in Table IV.

Test Instrumentation

The left and right motors and test transmission were equipped with speed, torque, temperature, and vibration sensors which were recorded as part of the facility data acquisition system. Lube system parameters such as temperature, oil pressure, and oil flow rate for the high and low pressure systems and clutch systems were also recorded. Facility data was collected at 5-Hz acquisition rate.

Figure 9 shows details of the facility vibration sensors. Six accelerometers were used, two mounted on each the left motor, test transmission, and right motor, in the vertical and horizontal directions. The accelerometers were broadband piezoelectric accelerometers with a nominal 11.5 pC/g charge sensitivity and linear frequency response from 1 to 8 kHz ± 1 dB. Overall root-mean-square (rms) vibration levels were measured from these accelerometers and collected as part of the facility data acquisition system.

Due to early sprag clutch development issues, proximity probes were installed on the low-speed output shaft drum to measure overall movement and run-out of the drum during steady state and speed shift conditions (Figure 10). The probes were eddy current proximity probes that provided output voltage directly proportional to the distance between the probe tip and the observed conductive surface (low-speed output shaft drum) and measured both static (position) and dynamic (vibration) values. The voltages were converted to distance (mils) using a static calibration process. Two probes were used. One was installed in the vertical position and one in the horizontal position. Typical range of measurement for the probes were 20 to 80 mils clearance between the probe tips and drum. Initial installed clearance between the probes and drum ranged from 35 to 50 mils. The measured results during operation were collected as part of the facility data acquisition system.

Figure 11 shows locations of installed thermocouples in the test transmissions. For both the OCG and DSI tests, thermocouples were installed on the input and output shaft duplex bearings. For the OCG tests, thermocouples were installed on the cluster duplex bearing. For the DSI tests, thermocouples were installed on all 12 planet gears bearings. The thermocouples were type J thermocouples. All were installed pressed against the bearing outer diameter using a spring-bolt attachment. The measured results during operation were collected as part of the facility data acquisition system.

Also shown in Figure 11 are three high frequency accelerometers that were installed inside the test transmissions. One was mounted on top of the input shaft duplex bearing housing and one on the output shaft duplex bearing housing. For the OCG tests, an accelerometer was mounted on top of the cluster shaft duplex bearing housing. For the DSI tests, an accelerometer was mounted on top of the planetary carrier. All were installed to measure vibration in vertical direction. The accelerometers were broadband high-frequency piezoelectric accelerometers with a nominal sensitivity of 10 mV/g and linear frequency response from 1 to 30 kHz ± 3dB. The outputs of the accelerometers along with tachometer pulses on the input and output shafts were routed to anti-aliasing filters with a 50 kHz cut-off frequency, then to a

separate PC-based data acquisition system. The data were acquired at 125 kHz sampling rate in 20-sec durations. Raw data were collected before, during, and after shifts for later post-processing.

Test Procedure

For the OCG test, the test transmissions as pictured in Figure 5 was built up on a bench then installed in the Glenn variable-speed transmission test facility. Upon installation, the lubrication system was initially checked. Oil pressures were adjusted and flow measurements were taken as shown in Table II. Green runs were initially performed on the test transmissions in which speeds and torques were gradually increased in order to break-in the parts and check operation of the test facility. The OCG was the first hardware to be tested and a number of facility issues were addressed during the start of testing (described later).

Once completed, the shift tests were performed to demonstrate feasibility of the OCG concept. The operation procedure for these tests was as follows. First, the lubrication system was started and the oil was heated to 160 °F. Upon reaching steady state, the transmission was run at the appropriate input speed of the test per speed control of the left motor. The right motor was set to power control at the appropriate level for the test. Upon reaching semi steady-state conditions, the clutch release profile was activated which linearly increased the clutch pressure from 0 to 400 psi at a rate of 20 psi/sec. At approximately 325 psi, the clutch disengaged and the transmission performed a high-to-low output speed shift. The low output speed condition (2:1 reduction ratio) was run for a short period of time, then the output load was reduced to zero. A clutch engagement profile was activated which linearly decreased the clutch pressure from 400 to 150 psi at a rate of 20 psi/sec. The clutch engaged at approximately 220 psi and the transmission performed a low-to-high output speed shift. These tests were run at 5,000, 8,000, 10,000, 12,500, and 15,000 rpm input speed. For these tests, facility data was continuously saved at 5 kHz. High-frequency vibration data was saved in 20-sec bursts.

After completion, the OCG was removed, disassembled, and inspected. The DSI configuration as pictured in Figure 8 was then installed. The lubrication system was checked and flow measurements were taken (Table IV). Green runs were performed and the same shifts tests as performed for the OCG were then repeated for the DSI configuration. After completion, additional tests were performed on the DSI configuration. The effects of clutch pressure ramp rate and right motor control mode on shifting characteristics were studied. Clutch pressure ramp rates of 20, 4, and 1 psi/sec were each performed for right motor control modes of power, torque, and manual control.

Results and Discussion

OCG Test Results

Shift tests were performed on the OCG transmission for input speeds of 5,000, 8,000, 10,000, 12,500, and 15,000 rpm. Transmission output speeds and corresponding shift clutch pressures for the OCG tests to characterize the shifting dynamics are given in Figure 12. Plotted are the output speeds (red lines, right vertical axis scale) and clutch pressures (blue lines, left vertical axis scale) versus run time for the shifts at 5,000, 8,000, 10,000, 12,500, and 15,000 rpm input speed. In order to align the plots for comparison, the horizontal-axis run times were defined as follows. For the high-to-low speed shift segments, the output speed started ramp-down at 20 sec. For the low-to-high speed shift segments, the output speed started ramp-up at 100 sec.

For each high-to-low speed shift test, the clutch disengagement profile started at approximately 5 sec on the plots. By 12 to 15 sec, the clutch pressures were linearly increasing. At 25 sec, the clutch reached

400 psi. Between 21 and 22 sec, the clutch exhibited momentary drops in pressure. These were caused by the full disengagement of the shift clutch where the applied oil fluid pressure overcame the spring engagement pressure in the clutch. Before the pressure drop, the clutch appeared to slip and the output speed started to decrease. After the drop, the clutch was fully disengaged and the output speed coasted down to half speed until engaged by the sprag. It is interesting to note that the time of the pressure drops did not occur the same for the different tests. It appears less slipping occurred at higher input speeds. For each low-to-high speed shift tests, the clutch engagement profile started at approximately 90 sec on the plots. At 100 sec, the clutch exhibited momentary increases in pressure. Here, the spring engagement force overcame the oil fluid pressure and the output speed started to increase until reaching full input speed which is when the clutch was fully engaged.

Table V summarizes the ramp-down and ramp-up time characteristics. Shown are ramp times (sec) and rates (rpm/sec). Ramp-down rates for shift tests from 5,000 to 12,500 rpm input speed steadily increased with input speed, then suddenly dropped at 15,000 rpm input speed. Ramp-up rates were similar for input speeds of 5,000 to 10,000 rpm and slightly higher for speeds of 12,500 and 15,000 rpm.

Figure 13 shows the transient input and output torques for the OCG shift tests. As with Figure 12, the horizontal axis is defined for start of the high-to-low output speed drop at 20 sec and start of the low-to-high speed increase at 100 sec. The left column is input torque for the complete shifts and the right column is the output torque for the complete shifts. As previously stated, the OCG transmission coasts down in speed after clutch disengagement during the high-to-low speed shift. Figure 13 shows the corresponding drops in torque starting at 20 sec during these coast downs. As the sprag is engaged the input torques increases back to their original values and the output torques increase to approximately twice their original values due to the system being set in power control. Table VI depicts the average measured output torques during the high-to-low speed shift tests, before and after shifts, as well as the peaks. It was originally desired to perform all the shift tests at the same torque level. Shifts at 5,000, 8,000, and 10,000 rpm were all run at the same approximate input torque level (Figure 13(a) to (f)). It was found, however, that transient overloads occurred at higher speeds during sprag engagement. Because of this, the output power set point was decreased with increased input speed in order to prevent test transmission overload (facility shutdown limits were set at 70 ft-lb torque). This is shown in the reduced power set points and resulting output torques at higher speeds in Table VI. One other point to mention is that the peak values listed in Table VI are from unfiltered 5-Hz facility data, where the data plotted in Figure 13 are filtered values, thus not reflecting the true peaks.

From very early shift attempts, it was discovered that a significant transient torque spike occurred at the start of clutch engagement for the low-to-high speed shift tests. This was due to the system trying to quickly speed up the output shaft during engagement. Because of this, the applied torque was set to zero for these tests in order to prevent transmission overload. Table VII depicts the average measured torques for the low-to-high speed shifts, before and after shifts, as well as the peaks. Even under no applied load, significant transient torque spikes occurred during the transitions. As with Table VI, peak values listed are from unfiltered data. Figure 12 and Figure 13 and Table V to Table VII characterized the transient speeds and torques of the OCG shifting dynamics. The transmission successfully shifted at its full design input speed of 15,000 rpm. But due to transient torque spikes, shifts were limited in applied torque levels in order to prevent overloads on the transmission. It is believed that the relative lack of appreciable slippage of the dry shifting clutch at these operating conditions and clutch pressure profiles (20 psi/sec ramp rate) was a major cause of the transient torque spikes. It should also be noted that the transmission was not initially designed to shift under much applied torque.

To further characterize the results of the OCG testing, additional transmission parameters are presented in Figure 14 to Figure 17. In these plots the data from all input speeds test are plotted

continuously on the horizontal axes. The input speeds for each shift are shown in the first graph of the plots as a reference. The parameters are color coded to indicate reduction ratio. Data at 1:1 output speed (high-speed) are shown in blue. Data at 2:1 output speed reduction (low-speed) are shown in red. The main purpose of the plots are to show the effect of reduction ratio on these parameters. It is not intended to show shift transients as was done with Figure 12 and Figure 13.

Transmission lubrication oil flow rates and inlet oil pressures are shown in Figure 14 for the OCG shift tests. Occasional drops in oil flow rate (Figure 14(b)) and corresponding spikes in oil inlet pressure (Figure 14(c)) occurred during the low-speed output regime. The cause is believed to be due to the occasional blocking of flow in the sprag clutch. The sprag clutch had four oil feed holes in its inner race, four oil exit holes in its outer race, and 16 sprag elements. Since the number of holes was an even divisor of the number of elements, it was possible for the elements to align with the holes and temporarily block oil flow. The mean oil flow rate at the low-speed output conditions did not appear to be affected by input speed, whereas the mean flow rate at the high-speed output decreased with input speed. This was also probably related to sprag clutch oil blockage.

Figure 15 shows transmission temperatures for the OCG shift tests. The forward and aft OCG cluster gear duplex bearing temperatures are shown in Figure 15(b). The transmission was not run long enough at each condition to achieve fully steady state results. One can see, however, an increase in temperature with input speed. Also, a very slight decrease in temperature occurred at the start of each low-speed output shift. The forward and aft bearings were very similar in response, with the forward bearing running slightly hotter. Figure 15(c) shows temperatures of the input and output shaft duplex bearings. As with the cluster, the bearing temperatures increased with increased input speed. The output shaft bearing showed a significant decrease in temperature at the low-speed output conditions due to the reduced shaft speed, and thus, reduced speed of the bearing.

Figure 16 shows the vibration from the facility accelerometers (from Figure 9) for the OCG shift tests. For the most part, the motor vibrations were fairly constant throughout the tests and not affected by test transmission reduction ratio (Figure 16(b), (e), and (f)). The motor vibrations slightly increased with speed and were largest at the highest tested speed condition (15,000 rpm). The OCG transmission vibration significantly increased at 8,000 rpm input speed (Figure 16(c) and (d)). The cause of this is unknown. Other than that, the OCG vibrations were fairly constant for the tests with a slight increase with input speed and a slight increase at the low-speed output regime.

Figure 17 shows the low-speed output shaft drum movement for the OCG shift tests as measured by the proximity probes. Shown is the measured clearance between the horizontal probe tip and shaft drum (Figure 17(b)) and the measured clearance between the vertical probe tip and shaft drum (Figure 17(c)). As seen from the figure, a significant difference in clearance occurred when comparing tests at 1:1 and 2:1 output speed. At 1:1 ratio, the low-speed output shaft drum is unloaded. At 2:1 ratio, torque flows through the drum. Thus, the position of the drum was affected by reduction ratio and torque flow path. This is further evident in the orbit plots of Figure 18. Here, the vertical and horizontal clearances in Figure 17 are converted to vertical and horizontal positions and plotted against each other in orbit plots. Data from the five different input speed conditions are divided into separate plots. Again, the plots clearly show a shift in shaft drum position when comparing 1:1 to 2:1 ratio test results. Also evident is reduced drum position oscillation at the higher tested input speeds of 12,500 and 15,000 rpm.

Measurement results of the high-frequency vibration of the OCG cluster gear bearing housing (from accelerometer 2 in Figure 11) are shown in Figure 19. Shown are raw time trace plots in 0.10-sec snapshots of the high-to-low speed OCG shift tests for each of the five input speeds tested. As stated before, data were sampled at 125 kHz. The left column are results before the shift (1:1 ratio output speed) and the right column are results after the shift (2:1 ratio output speed). Since the accelerometers were

mounted directly on the duplex bearing housing inside the transmission, the vibration levels were relatively high. Also, the accelerometer digitizing range was mistakenly set too low and signal clipping occurred at ± 125 G's. Before the shift (left column), the OCG cluster was unloaded. Impulse spikes at the OCG cluster shaft and input shaft periods can be seen. After the shift (right column), the torque was transmitted through the OCG cluster and the vibration levels significantly increased. Significant impulse spikes at the cluster period occurred at 12,500 rpm input speed and somewhat at 15,000 rpm.

Fast Fourier transforms of the time traces are shown in Figure 20. The spectra were based on 5 sec of vibration data using a Hanning window and 32,768 points (3.8 Hz bandwidth) per spectrum resulting in 19 frequency averages per plot. Again, the left column are results before the shift (1:1 ratio output speed) and the right column are results after the shift (2:1 ratio output speed). Table VIII gives shaft and gear mesh frequencies for the OCG configuration at the various input speeds tested. Comparing this with Figure 20, the major vibration energy occurred at the gear mesh fundamental (and somewhat two times the gear mesh fundamental) frequencies. Also, as with Figure 18, vibration levels significantly increased after shift, which was when the OCG was loaded.

DSI Test Results

As with the OCG, shift tests were performed on the DSI planetary transmission for input speeds of 5,000, 8,000, 10,000, 12,500, and 15,000 rpm. Transmission output speeds and corresponding shift clutch pressures for the DSI tests to characterize the shifting dynamics are given in Figure 21. As with Figure 12 and Figure 13 from the OCG tests, the horizontal axis is defined for start of the high-to-low output speed drop at 20 sec and start of the low-to-high speed increase at 100 sec. The results of speed, clutch pressure, and clutch pressure drops, are very similar to those from the OCG tests. Table IX summarizes the ramp-down and ramp-up time characteristics. The overall results are also very similar to those from the OCG tests.

Figure 22 shows the transient input and output torques for the DSI shift tests. As with speed, the DSI torque transients were very similar to that from the OCG tests. Table X depicts the average measured output torques during the high-to-low speed shift tests. Table XI depicts the average measured torques for the low-to-high speed shifts. The peaks during the shift transients were a little erratic, but in general, matched those from the OCG tests. All test set points were identical for both the OCG and DSI tests with one exception. The set point power for the DSI tests at 12,500 rpm input speed was 22 hp, where the set point power for the OCG tests at 12,500 rpm input speed was 38 hp. The lower set point was used due to torque limit exceedance experienced at attempts at 38 hp during DSI testing. In summary, the DSI planetary transmission successfully shifted at its full design input speed of 15,000 rpm. As with the OCG, shifts were limited in applied torque levels in order to prevent overloads on the transmission. Since the transient behavior of the OCG and DSI tests were very similar, it is deduced that the shift clutch (same dry carbon clutch used with both configurations) had more of an effect on dynamics than the reduction gearing configuration itself.

Transmission lubrication oil flow rates and inlet oil pressures are shown in Figure 23 for the DSI shift tests. As seen from the initial oil flow measurements (Table II and Table IV), the overall oil flow rate of the DSI was greater than that for the OCG due to the increased number of jets to the planetary gears and bearings. As with the OCG tests, drops in oil flow rate (Figure 23(b)) and corresponding spikes in oil inlet pressure (Figure 23(c)) occurred during the low-speed output regime. The drops appeared more frequently compared to the OCG tests, and the frequency increased with input speed. The cause of the difference in flow drops between the DSI and OCG is not completely known, but may be related to the additional backup bearing used in the DSI sprag assembly, causing an additional restriction to the oil flow. As with

the OCG tests, the mean oil flow rate at the low-speed output conditions was not affected by input speed, whereas the mean flow rate at the high-speed output decreased with input speed.

Figure 24 shows transmission temperatures for the DSI shift tests. Temperature of all 12 DSI planet bearings were recorded. The hottest bearing of the 12 was the idler #3 aft bearing. The coolest was the star #3 forward bearing. Both of these temperatures are shown in Figure 24(b). All 12 bearings exhibited similar trends and were banded within the two depicted in Figure 24(b). One concern related to the DSI design was the extremely high speed of the planet gears and bearings. Table XII gives the speeds of the planetary components. As seen the table, the star planets run up to 39,474 rpm at full input speed. Even though the transmission was not run completely to steady state, the measured planet bearing temperatures were reasonable considering the speed at which they operated. The DSI planet bearings were significantly hotter than the OCG cluster bearings due to their increased operating speed and possible insufficient oil drainage provisions.

Figure 24(c) shows temperatures of the input and output shaft duplex bearings. As with the planets, the bearing temperatures increased with increased input speed. The output shaft bearing showed a significant decrease in temperature at the low-speed output conditions due to the reduced shaft speed, and thus, reduced speed of the bearing. The duplex bearings, in general, behaved similar to those for the OCG tests.

Figure 25 shows the vibration from the facility accelerometers (from Figure 9) for the DSI shift tests. The motor vibrations were fairly constant throughout the tests and not affected by test transmission reduction ratio (Figure 25(b), (e), and (f)). The DSI transmission vibration slightly increased with input speed (Figure 25(c) and (d)). The DSI transmission vibration was higher at 2:1 output compared to 1:1 for 5,000, 8,000, and 10,000 rpm input speeds, but were lower at 2:1 for speed of 12,500 and 15,000 rpm.

Figure 26 shows the low-speed output shaft drum movement for the DSI shift tests as measured by the proximity probes. Figure 27 shows the corresponding orbit plots. As seen from the figures, the position of the drum did not show a shift in shaft drum position when comparing 1:1 to 2:1 ratios test results. Thus, the sprag backup bearing was successful in locating the shaft drum. Also, the overall movement of the drum was lower with the backup bearing installed when comparing results from Figure 27 and Figure 18.

Measurement results of the high-frequency vibration of the DSI planetary carrier (from accelerometer 2 in Figure 11) are shown in Figure 28. Shown are raw time trace plots in 0.10-sec snapshots taken at 125 kHz sample rate of the high-to-low speed DSI shift tests for each of the five input speeds tested. The vibration levels were relatively high but lower than those from the OCG cluster gear housing. The accelerometer digitizing range was mistakenly set too low and signal clipping occurred at ± 125 G's for tests at input speeds 5,000 to 12,500 rpm. This was corrected and no clipping occurred for the test at 15,000 rpm. The vibration levels for the loaded planetary (after shift, right column) were significantly higher than those for the unloaded planetary (before shift, left column). Significant impulse spikes at the output shaft period occurred for tests at 10,000 and 12,500 rpm input speed.

Fast Fourier transforms of the time traces are shown in Figure 29. As with the OCG analysis, the spectra were based on 5 sec of vibration data using a Hanning window and 32,768 points (3.8 Hz bandwidth) per spectrum resulting in 19 frequency averages per plot. Again, the left column are results before the shift (1:1 ratio output speed) and the right column are results after the shift (2:1 ratio output speed). Table XII gives shaft and gear mesh frequencies for the DSI configuration at the various input speeds tested. Comparing this with Figure 29, the major vibration energy occurred at the planetary gear mesh frequencies. Also, as with Figure 28, vibration levels significantly increased after shift which was when the DSI planetary was loaded.

Additional shift tests were performed on the DSI transmission to determine the effect of clutch pressure ramp rate and right motor control mode on the shifting characteristics. Clutch pressure ramp rates of 20, 4, and 1 psi/sec were each performed for right motor control modes of power, torque, and manual control. Figure 30 gives the output speed and clutch pressure and Figure 31 gives the input and output torques for shifts using power control mode. Figure 32 gives the output speed and clutch pressure and Figure 33 gives the input and output torques for shifts using torque control mode. Figure 34 gives the output speed and clutch pressure and Figure 35 gives the input and output torques for shifts using manual control mode. Table XIII summarized the output speed ramp times and rates as well as output torques for the high-to-low shifts of all these tests. Table XIV gives the output speed ramp times and rates as well as output torques for the low-to-high shifts of all these tests. Figure 36 depicts the speed ramp times, rates, and peak output torques. Note that all tests were performed at 5,000 rpm input speed. For the high-to-low shifts, the set points for all tests were adjusted to produce the approximate same amount of applied output torque before shift. For all low-to-high speed shifts, the applied torque was set to zero in order to prevent transient overloads (right motor, manual mode, 0 percent).

From Table XIII and Table XIV and Figure 36, low-to-high shift output speed ramp-up times were less than high-to-low shift output speed ramp-down times for the same control and clutch pressure ramp rate. Low-to-high speed ramp-up times were governed by the relatively quick engagement of the dry clutch. High-to-low ramp-down times were basically a coast down of the output shaft, and thus, had longer ramp-down times compared to ramp-up times. For the low-to-high speed shifts, the output speed ramp-up time slightly decreased as the clutch pressure ramp-down rate increased. This was caused by slightly less clutch slippage as the clutch pressure ramp-down rate increased. For the high-to-low speed shifts, open-loop manual control mode produced larger speed ramp-down times compared to closed-loop power and torque control modes, while power and torque control mode ramp-down times were similar to each other. This was caused by the following. At the start of the high-to-low speed shifts, the output shaft coasted down in speed which resulted in a reduction in torque (Figure 31, Figure 33, and Figure 35). Since the torque levels decreased, a corresponding increase in load motor current was produced under closed-loop control, which produced more drag in the load motor and a decrease in ramp-down time compared to that using open-loop manual control.

As previously stated, all low-to-high shift tests were performed unloaded. For these tests, the peak output torque increased as the clutch pressure ramp-down rate increased. Again, this was due to slightly less clutch slippage with increased clutch pressure ramp-down rate. Even at low clutch pressure ramp-down rates, a relatively small amount of clutch slippage occurred for the dry clutch configuration. This produced transient torque spikes during low-to-high speed shifts, and thus, prevented operation of low-to-high speed shifts under any appreciable applied torque. For the high-to-low shift tests, the peak output torque was the same for all clutch pressure ramp-up rates for power control mode. Other than that, there was no other trend in peak output torque with clutch pressure ramp-up rates or control modes for the high-to-low shifts.

Lessons Learned

The testing described in this current study was performed in the newly developed NASA Glenn Research Center variable-speed transmission test facility. A number of facility development issues were encountered during initial testing of the first transmission tested, the OCG configuration. Details of various lessons learned are described in (Ref. 14). A summary of these results are as follows.

The first was failure of the output shaft coupling (Figure 37). The facility uses commercially available high-speed, metal bellows couplings between the test transmission and left (driver) and right (loader) motors. The couplings employ taper lock hubs which are tightened together to lock connecting shafts

together. Due to requirements of rather small shaft diameters in the test transmission, intermediate sleeves were needed in between the shaft and coupling assembly. It is believed these sleeves lowered the torque capacity of the coupling from that stated in the manufacturers data sheets. During initial testing of the OCG configuration, unexpected transient overloads were encountered. These transient torque spikes contributed to coupling slippage, which reduced the torque through the output shaft. The facility was in closed-loop torque control mode at the time, and thus, issued a reversing rotation to the right motor to increase torque. Excessive slippage, spinning, and eventual scoring of the shaft surfaces were encountered. The issue was resolved by limiting the allowed torque to 70 ft-lb through use of facility shutdowns and eventually incorporating keys in the connections.

The second issue encountered was failure of a sprag clutch (Figure 38). The sprag shown in this figure was a high capacity clutch with 34 sprag elements. It is believed that insufficient lubricant flow was used in this condition, as the clutch failed during overrunning (1:1 ratio output speed) operation. It is believed that only 0.2 gpm oil flow rate was used in this test. The issue was resolved by increasing the flow rate to 0.9 gpm and using a sprag with 16 (instead of 34) elements. In addition, a backup sprag support bearing was added in later testing to further control the position of the low-speed output shaft drum. The aft sprag bearing and spider bearing (located radial between low-speed shaft and input shaft, Figure 6) form a duplex-bearing support, which properly supports both the low-speed shaft and sprag, and is also axially preloaded. With this, all shafts have duplex bearing support.

The original dry carbon-carbon clutch was a commercially available clutch used in the automotive racing industry. It had excessive torque capacity, but required a high release force to disengage the clutch. The original design included two diaphragm (conical) springs with integral machined radial fingers mounted in series for disengagement. The two springs provided the rated capacity but required an oil pressure of approximately 700 psi applied to the piston to release the fingers and disengage the clutch. Sealing issues were encountered with the above when trying to provide the excessively high oil pressure. The clutch was then modified by removing one diaphragm spring and installing correction shims. This modification reduced the clamping rated capability yet provided adequate clamping force and required less force (oil pressure) to release the clutch. The resulting design is shown in Figure 39.

As previously mentioned, both transmission configurations successfully shifted at their full design input speed of 15,000 rpm, but due to transient torque spikes, were limited in applied torque levels in order to prevent overloads on the transmission. It is believed that the relative lack of appreciable slippage of the dry shifting clutch at operating conditions and pressure profiles tested was a major cause of the transient torque spikes. A second configuration, a wet clutch, has been designed and fabricated and is shown in Figure 40. The wet clutch contains sets of steel-friction plates as used in automotive applications. The steel plates are attached to the input shaft through their outer diameters. The friction plates are attached to the inner shaft through their inner diameters. Upon assembly, the plates are locked together through use of drive springs, thus locking the input shaft to the clutch inner shaft. To disengage the clutch, pressurized oil is applied to the piston, which pushes on the springs to separate the clutch plates. The separated clutch plates are kept cool and lubricated through use of the oil system used to lubricate the gears and bearings in the test transmission, which is independent of the above clutch control circuit. The required pressure to release the wet clutch is significantly lower than that of the dry clutch due to the increased cross-sectional area of the wet clutch piston. Initial bench testing of the wet clutch resulted in a required release pressure of approximately 140 psi, compared to 325 for the dry clutch. It is believed that the reduced required release pressure along with the wet clutch characteristics will allow better control of slippage to address the transient torque spikes. Future shifts tests with the wet clutch configuration are planned.

Lastly, as mentioned, issues where encountered in the oil transfer region to maintain adequate oil pressure to the shift clutch. The initial design used cast iron oil transfer seal rings, as used in commercial automotive transmissions. These seal rings exhibited excessive wear during high speed and high pressure operation (Figure 41). The rings were replaced with DuPont Vespel polyimide material and exhibited much improved wear rates.

Conclusions

Experimental tests were performed on two promising two-speed transmission configurations designed for use in advanced rotorcraft application: 1) the offset compound gear (OCG) transmission, and 2) the dual star/idler (DSI) planetary transmission. Testing was performed in the NASA Glenn Research Center variable-speed transmission test facility. Shift tests were performed on the transmissions at input speeds of 5,000, 8,000, 10,000, 12,500, and 15,000 rpm. Speed and torque transients as well as transmission component characteristics were collected. The following results were obtained:

1) Both the OCG and DSI configurations successfully perform speed shifts at full rated 15,000 rpm input speed.

2) The transient shifting behavior of the OCG and DSI configurations were very similar. Since the same shift clutch was used in both configurations, it was deduced that the shift clutch had more of an effect on shifting dynamics than the reduction gearing configuration itself.

3) For both OCG and DSI configurations, low-to-high speed shifts were limited in applied torque levels in order to prevent overloads on the transmission due to transient torque spikes. It is believed that the relative lack of appreciable slippage of the dry shifting clutch at operating conditions and pressure profiles tested was a major cause of the transient torque spikes.

4) For low-to-high speed shifts with the DSI configuration, the output speed ramp-up time slightly decreased and the peak out torque slightly increased as the clutch pressure ramp-down rate increased. This was caused by slightly less clutch slippage as the clutch pressure ramp-down rate increased.

5) The planet bearings in the DSI configuration successfully operated at high speed during test.

References

1. Johnson, W., Yamauchi, G.K., and Watts, M.E., “NASA Heavy Lift Rotorcraft Systems Investigation,” NASA/TP—2005-213467, 2005.
2. Acree, C.W., Yeo, H., and Sinsay, J.D., “Performance Optimization of the NASA Large Civil Tiltrotor,” International Powered Lift Conference, London, UK, Jul. 22-24, 2008.
3. Goi, T., Kawakami, K., Yamakawa, E., and Tanaka, H., “Variable Rotor Speed Transmission with High Speed Traction Drive,” American Helicopter Society 55th Annual Forum, Montreal, Quebec, Canada, May 25-27, 1999.
4. Handschuh, R.F., and Zakrajsek, J.J., “Current Research Activities in Drive System Technology in Support of the NASA Rotorcraft Program,” American Helicopter Society Vertical Lift Aircraft Design Conference, San Francisco, CA, Jan. 18-20, 2006.
5. Ai, X., Mohr, T., and Anderson, S., “An Electro-Mechanical Infinitely Variable Speed Transmission,” SAE 2004 World Congress, Detroit, MI, Mar. 8-11, 2004.
6. Saribay, Z., Smith, E., Lemanski, A., Bill, R., Wang, K.W., and Rao, S., “Compact Pericyclic Continuously Variable Speed Transmission Systems: Design Features and High-Reduction Variable Speed Case Studies,” American Helicopter Society 63nd Annual Forum, Virginia Beach, VA, May 1-3, 2007.

7. Harris, F. D., “An Overview of Autogyros and the McDonnell XV-1 Convertiplane,” NASA/CR—2003-212799, 2003.
8. Munter, P. L., “Design and fight test of a two-speed helicopter transmission,” American Helicopter Society 10th Annual Forum, Washington, D.C., May 24-26, 1954.
9. Lentine, F. P., G. W. P. and Oglesby, T. H., “Research in maneuverability of the XH-51A compound helicopter,” USAAVLABSTR Technical Report 68-23, U.S. Army Aviation Materiel Laboratories, Fort Eustis, VA, Jun. 1968.
10. Karem, A., “Hummingbird A160 and optimum speed rotor (OSR),” AHS International Specialists’ Meeting - Unmanned Rotorcraft: Design, Control and Testing, Proceedings, Phoenix, AZ, Jan. 18-20, 2005.
11. Brown, F., Robuck, M., Kaiser, E., Ohlerking, W., Schellhase, E., Mychalowicz, E., and Paul, D., “Design and Development of a Dual Ratio Transmission for the A160T UAV Rotorcraft,” American Helicopter Society 66th Annual Forum, Phoenix, AZ, May 11-13, 2010.
12. Stevens, M.A., Handschuh, R.F., and Lewicki, D.G., “Concepts for Variable/Multi-Speed Rotorcraft Drive System,” American Helicopter Society 64th International Forum, Montreal, Canada, Apr. 29 - May 1, 2008.
13. Stevens, M.A., Handschuh, R.F., and Lewicki, D.G., “Variable/Multispeed Rotorcraft Drive System Concepts,” NASA/TM—2009-215456, Army Research Laboratory Report ARL-TR-4758, Mar. 2009.
14. Stevens, M.A., Lewicki, D.G., and Handschuh, R.F., “Concepts for Multi-Speed Rotorcraft Drive System - Status of Design and Testing at NASA GRC,” American Helicopter Society 71st Annual Forum and Technology Display, Virginia Beach, VA, May 5-7, 2015.
15. Stevens, M.A., Handschuh, R.F., and Lewicki, D.G., “Offset Compound Gear Inline Two-Speed Drive,” United Stated Patient No. 8,091,445 B1, Jan. 10, 2012.
16. Stevens, M.A., Handschuh, R.F., and Lewicki, D.G., “Offset Compound Gear Inline Two-Speed Drive,” United Stated Patient No. 8,668,613 B1, Mar. 11, 2014.

TABLE I.—BASIC GEAR DIMENSIONS FOR OCG TRANSMISSION CONFIGURATION

	Input gear	Cluster gear 1	Cluster gear 2	Output gear
Type	External	Internal	External	Internal
Number of teeth	25	37	31	42
Diametral pitch, teeth/in.	8.7273	8.7273	8.0000	8.0000
Pitch diameter, in.	2.8646	4.2396	3.8750	5.2500
OD (ext), ID (int), in.	3.0938	4.0850	4.1250	5.0000
Pressure angle, deg	20.0	20.0	20.0	20.0
Face width, in.	0.375	0.375	0.375	0.375

TABLE II.—OIL FLOW RATES AT 80 psi SUPPLY PRESSURE, 160 °F OIL INLET TEMPERATURE, FOR OCG TEST CONFIGURATION

Component	Flow rate, gpm
OCG duplex bearing	0.1
OCG gears	0.3
Output shaft duplex bearing	0.1
Input shaft duplex bearing	0.1
Sprag clutch	0.9

TABLE III.—BASIC GEAR DIMENSIONS FOR DSI TRANSMISSION CONFIGURATION

	Sun gear	Planet star gear	Planet idler gear	Ring gear
Type	External	External	External	Internal
Number of teeth	50	19	20	101
Diametral pitch, teeth/in.	12.0000	12.0000	12.0000	12.0000
Pitch diameter, in.	4.1667	1.5833	1.6667	8.4167
OD (ext), ID (int), in.	4.3101	1.7367	1.8101	8.2633
Pressure angle, deg.	20.0	20.0	20.0	20.0
Face width, in.	0.600	0.600	0.600	0.600

TABLE IV.—OIL FLOW RATES AT 80 psi SUPPLY PRESSURE, 160 °F OIL INLET TEMPERATURE, FOR DSI TEST CONFIGURATION

Component	Flow rate, gpm
DSI bearings	0.2
DSI gears	0.8
Output shaft duplex bearing	0.1
Input shaft duplex bearing	0.1
Sprag clutch	0.9

TABLE V.—OCG SHIFT TEST CHARACTERISTICS,
RAMP-DOWN AND RAMP-UP TIMES AND RATES

Shift no.	Input speed, rpm	Ramp down time, sec	Ramp down rate, rpm/sec	Ramp up time, sec	Ramp up rate, rpm/sec
1	5,000	3.4	742	2.0	1,280
2	8,000	4.6	869	3.2	1,244
3	10,000	5.6	903	3.8	1,304
4	12,500	6.0	1,044	4.2	1,511
5	15,000	10.0	747	4.8	1,557

TABLE VI.—OCG SHIFT TEST CHARACTERISTICS,
OUTPUT TORQUES FOR HIGH-TO-LOW SPEED SHIFTS

Shift no.	Set points		Output torque, ft-lb		
	Input speed, rpm	Output power, hp	Before shift	After shift	Peak
1	5,000	18	18.9	37.8	37.8
2	8,000	30	19.6	39.4	39.4
3	10,000	38	19.9	40.1	57.8
4	12,500	38	15.9	32.5	50.0
5	15,000	20	6.9	14.1	31.0

TABLE VII.—OCG SHIFT TEST CHARACTERISTICS,
OUTPUT TORQUES FOR LOW-TO-HIGH SPEED SHIFTS

Shift no.	Input speed, rpm	Output torque, ft-lb		
		Before shift	After shift	Peak
1	5,000	0.7	1.1	37.1
2	8,000	1.1	1.6	33.6
3	10,000	1.3	2.0	43.4
4	12,500	1.1	2.0	53.7
5	15,000	1.1	2.3	51.5

TABLE VIII.—OCG CONFIGURATION SHAFT AND GEAR MESHING FREQUENCIES

Speed, rpm			Shaft frequencies, Hz			Input mesh frequencies, Hz			Output mesh frequencies, Hz		
Input shaft	Cluster shaft	Output shaft	Input shaft	Cluster shaft	Output shaft	1X	2X	3X	1X	2X	3X
5,000	3,378	2,494	83	56	42	2,083	4,167	6,250	1,745	3,491	5,236
8,000	5,405	3,990	133	90	66	3,333	6,667	10,000	2,793	5,586	8,378
10,000	6,757	4,987	167	113	83	4,167	8,333	12,500	3,491	6,982	10,473
12,500	8,446	6,234	208	141	104	5,208	10,417	15,625	4,364	8,728	13,091
15,000	10,135	7,481	250	169	125	6,250	12,500	18,750	5,236	10,473	15,709

TABLE IX.—DSI SHIFT TEST CHARACTERISTICS,
RAMP-DOWN AND RAMP-UP TIMES AND RATES

Shift no.	Input speed, rpm	Ramp down time, sec	Ramp down rate, rpm/sec	Ramp up time, sec	Ramp up rate, rpm/sec
1	5,000	3.4	752	2.0	1,269
2	8,000	4.8	842	3.0	1,330
3	10,000	5.2	973	3.6	1,410
4	12,500	7.8	808	4.2	1,445
5	15,000	10.4	726	5.6	1,333

TABLE X.—DSI SHIFT TEST CHARACTERISTICS, OUTPUT
TORQUES FOR HIGH-TO-LOW SPEED SHIFTS

Shift no.	Set points		Output torque, ft-lb		
	Input speed, rpm	Output power, hp	Before shift	After shift	Peak
1	5,000	18	19.1	38.2	38.2
2	8,000	30	19.7	39.8	46.7
3	10,000	38	20.0	40.3	50.2
4	12,500	22	9.2	18.7	32.6
5	15,000	20	7.0	14.3	36.6

TABLE XI.—DSI SHIFT TEST CHARACTERISTICS, OUTPUT
TORQUES FOR LOW-TO-HIGH SPEED SHIFTS.

Shift no.	Input speed, rpm	Output torque, ft-lb		
		Before shift	After shift	Peak
1	5,000	1.0	1.1	36.5
2	8,000	1.1	1.7	34.7
3	10,000	1.1	1.9	53.4
4	12,500	1.1	2.2	51.9
5	15,000	1.0	3.0	44.7

TABLE XII.—DSI CONFIGURATION SHAFT AND GEAR MESHING FREQUENCIES

Speed, rpm				Frequencies, Hz		Gear mesh frequencies, Hz		
Input shaft	Planet star	Planet idler	Output shaft	Input shaft	Output shaft	1X	2X	3X
5,000	13,158	12,500	2,475	83	41	4,167	8,333	12,500
8,000	21,053	20,000	3,960	133	66	6,667	13,333	20,000
10,000	26,316	25,000	4,950	167	83	8,333	16,667	25,000
12,500	32,895	31,250	6,188	208	103	10,417	20,833	31,250
15,000	39,474	37,500	7,426	250	124	12,500	25,000	37,500

TABLE XIII.—EFFECT OF CONTROL MODE AND CLUTCH PRESSURE RAMP RATE ON SHIFT CHARACTERISTICS FOR DSI CONFIGURATION HIGH-TO-LOW SPEED SHIFTS

Shift no.	Control mode	Set point	Clutch pressure rate, psi/sec	Ramp down time, sec	Ramp down rate, rpm/sec	Output torque, ft-lb		
						Before shift	After shift	Peak
6	Power	18 hp	20	4.2	606	18.9	38.1	38.1
7	Power	18 hp	4	7.4	342	18.9	38.1	38.1
8	Power	18 hp	1	11.4	222	18.9	38.3	38.3
9	Torque	20 ft-lb	20	3.8	675	20.0	20.2	42.5
10	Torque	20 ft-lb	4	9.0	281	20.0	20.1	29.1
11	Torque	20 ft-lb	1	11.2	226	20.0	19.8	36.2
12	Manual	11 %	20	5.2	488	19.3	19.0	19.0
13	Manual	11 %	4	9.4	269	19.3	18.9	27.4
14	Manual	11 %	1	12.8	197	19.2	18.9	26.5

TABLE XIV.—EFFECT OF CONTROL MODE AND CLUTCH PRESSURE RAMP RATE ON SHIFT CHARACTERISTICS FOR DSI CONFIGURATION LOW-TO-HIGH SPEED SHIFTS

Shift no.	Control mode	Set point, %	Clutch pressure rate, psi/sec	Ramp up time, sec	Ramp up rate, rpm/sec	Output torque, ft-lb		
						Before shift	After shift	Peak
6	Manual	0	20	2.0	1,266	1.1	1.2	39.6
7	Manual	0	4	2.6	982	0.7	0.9	29.9
8	Manual	0	1	3.2	762	0.8	1.1	24.2
9	Manual	0	20	2.0	977	0.9	1.1	35.1
10	Manual	0	4	2.6	946	0.9	1.1	30.5
11	Manual	0	1	3.2	767	0.6	0.9	26.7
12	Manual	0	20	2.0	1,246	0.7	0.9	35.5
13	Manual	0	4	2.4	1,052	0.9	1.2	32.5
14	Manual	0	1	3.0	831	0.9	1.2	28.1

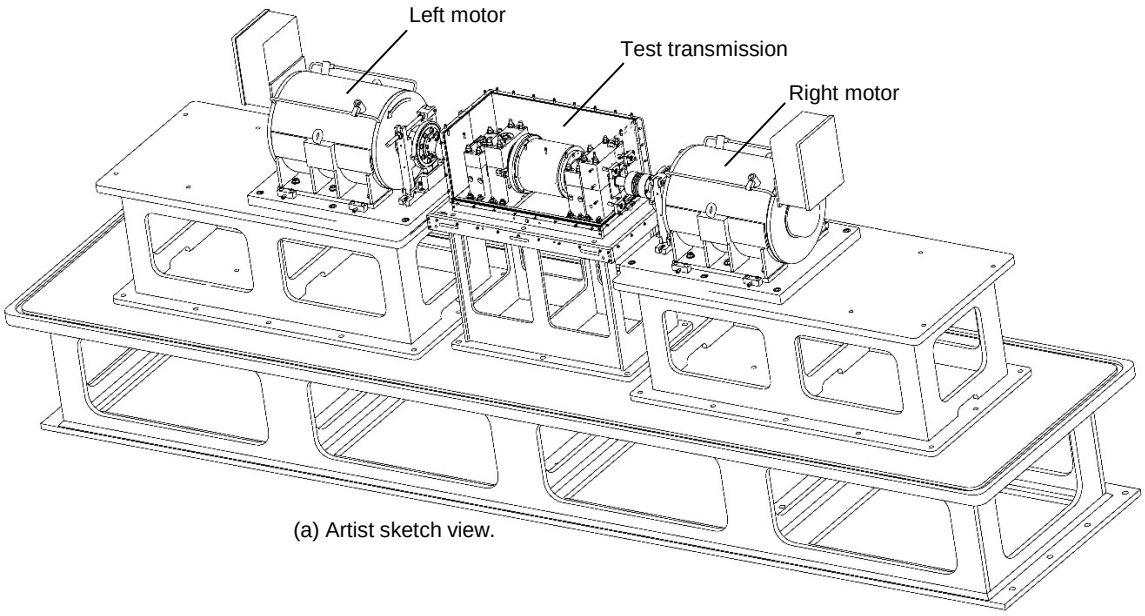

(a) Artist sketch view.

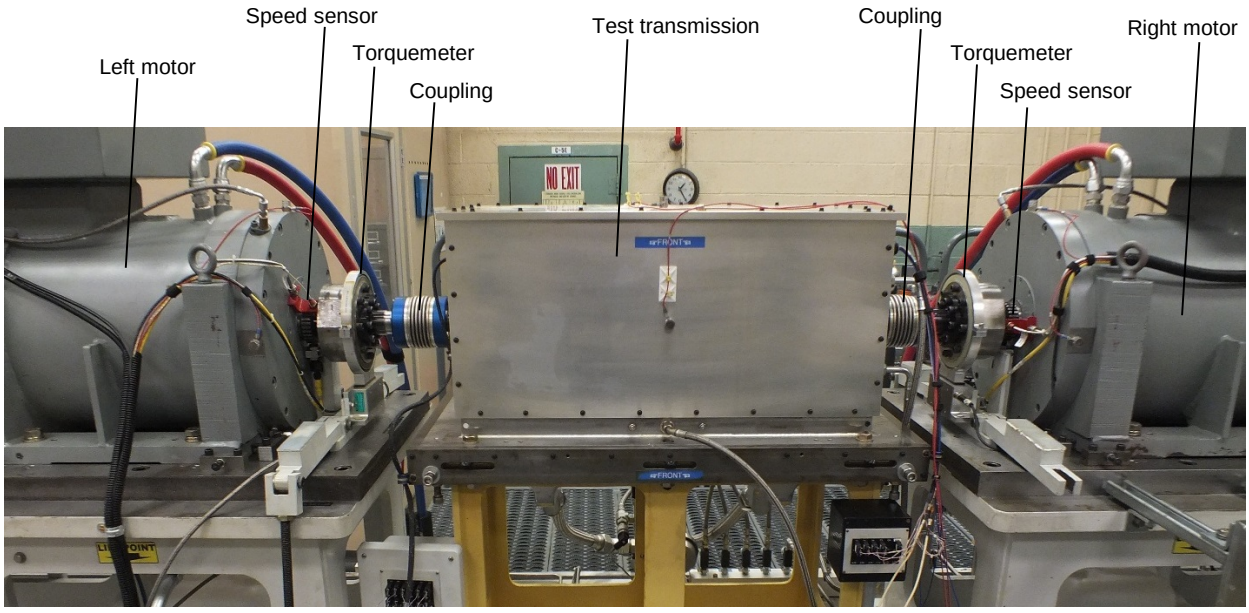

(b) Photo view.

Figure 1.—NASA Glenn Research Center variable-speed transmission test facility.

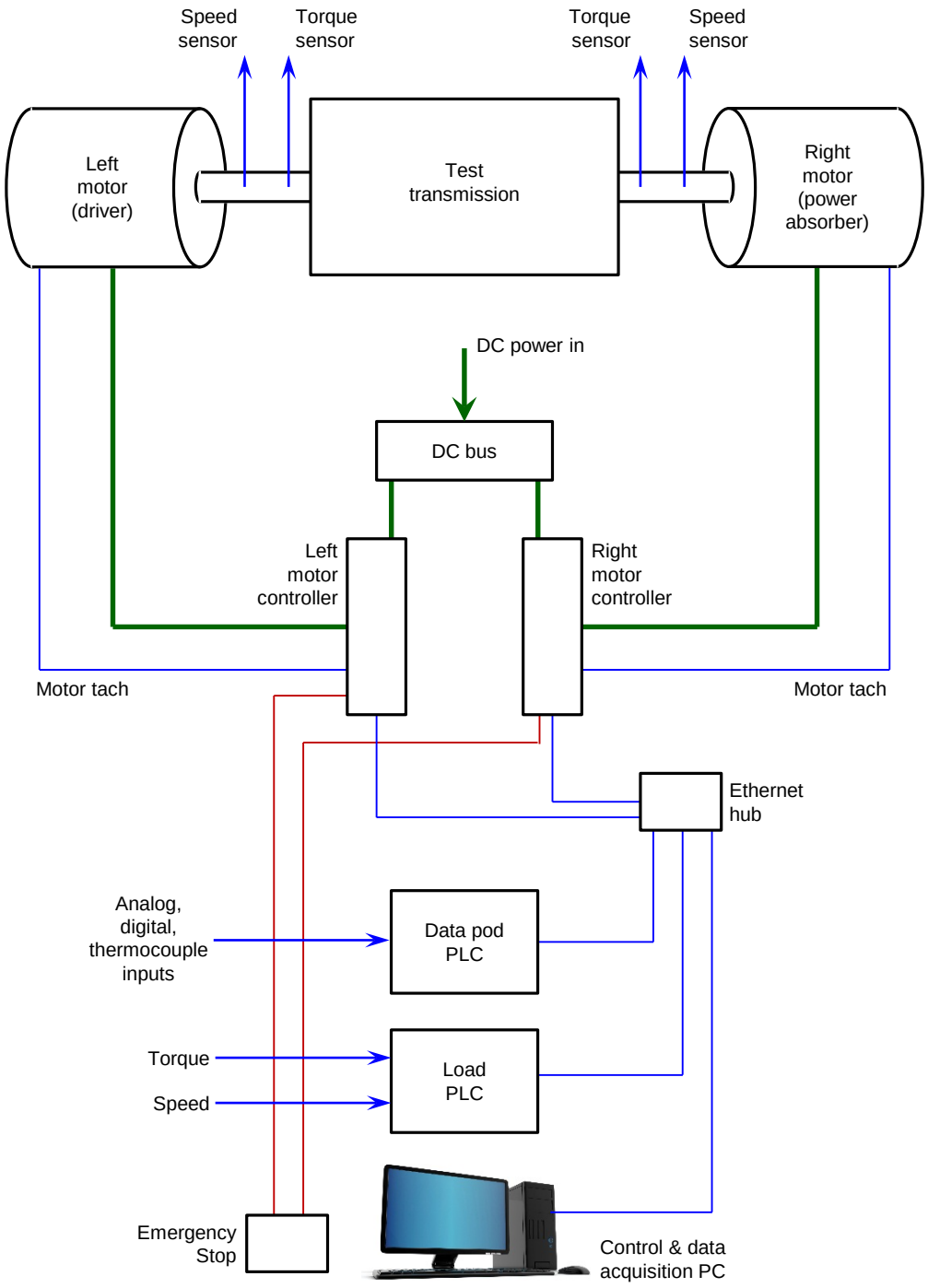

Figure 2.—Variable-speed transmission test facility control system.

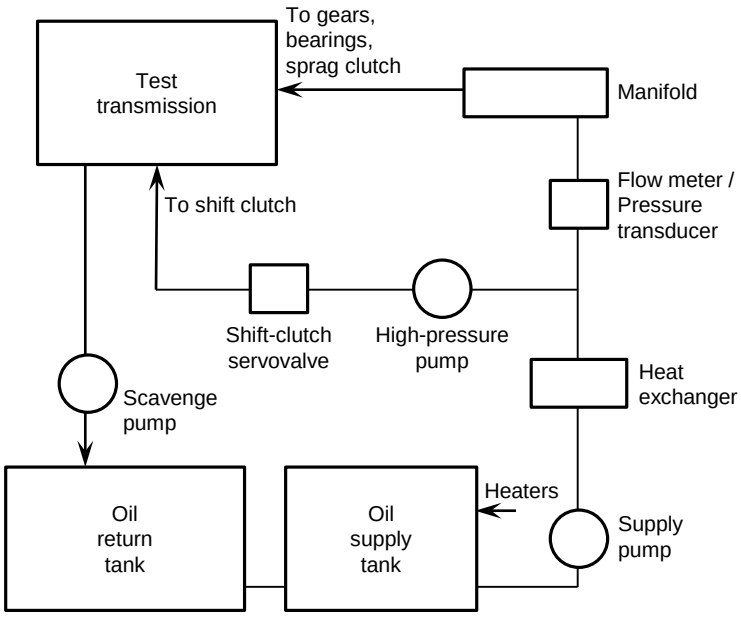

Figure 3.—Test transmission oil lubrication system.

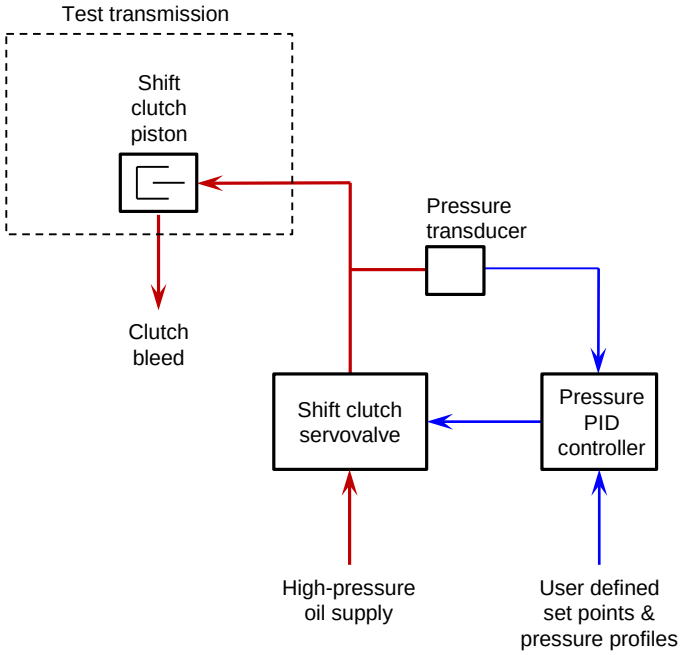

Figure 4.—Shift clutch pressure control system.

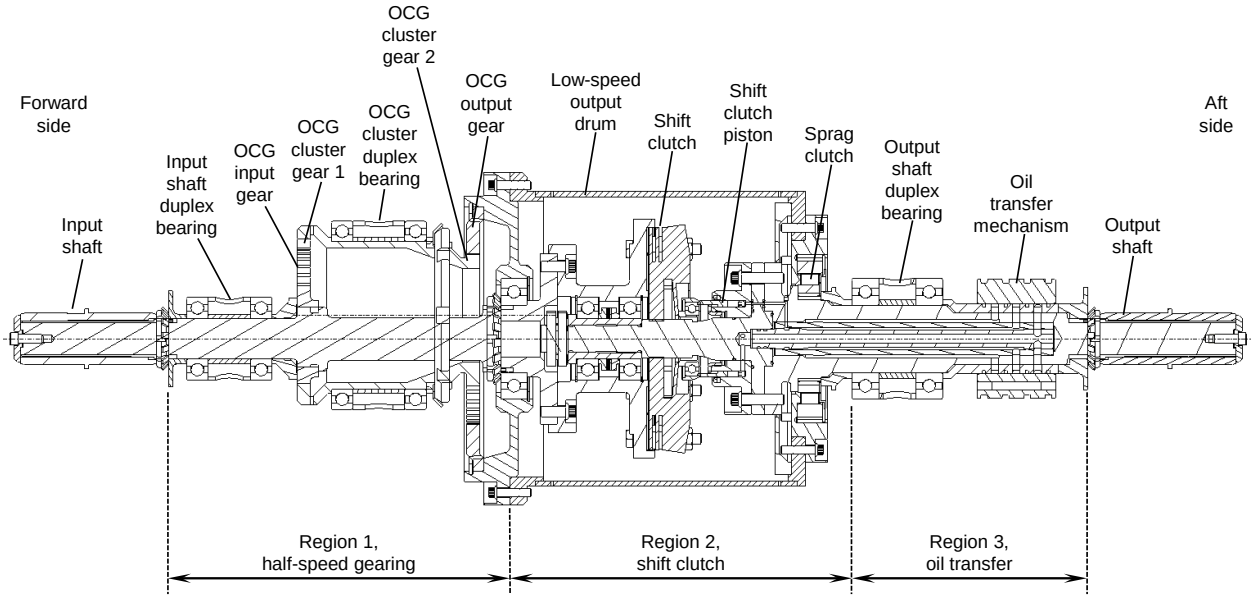

(a) Cross-sectional view.

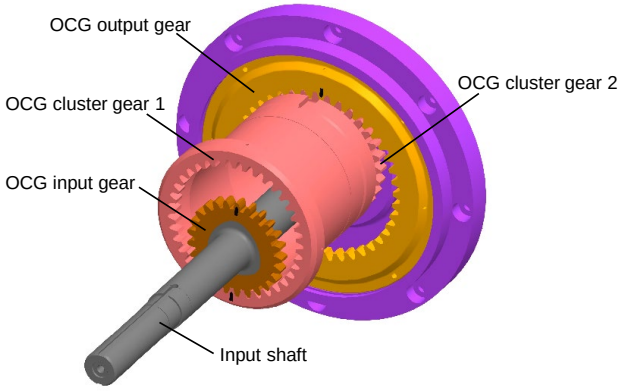

(b) 3D view of OCG gearing (region 1).

Figure 5.—Offset compound gear (OCG) transmission configuration.

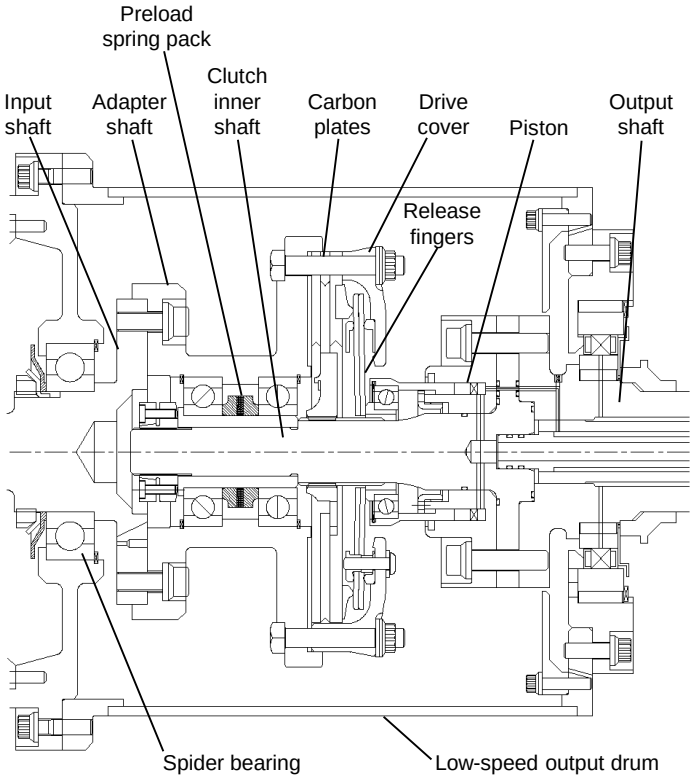

Figure 6.—Dry shift clutch.

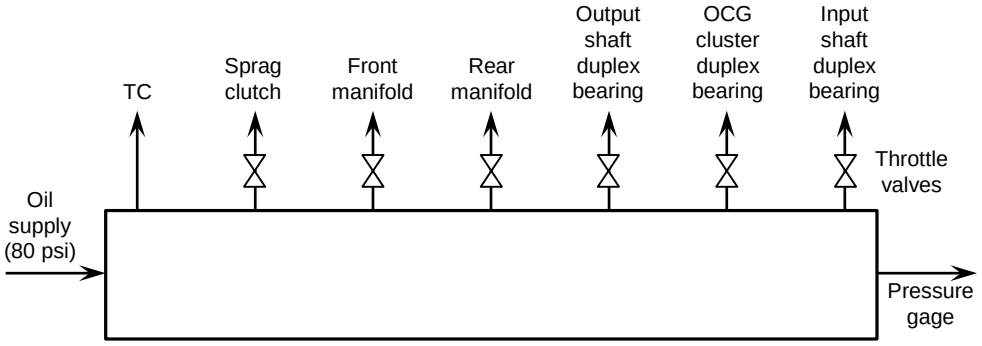

Figure 7.—Test transmission oil supply manifold.

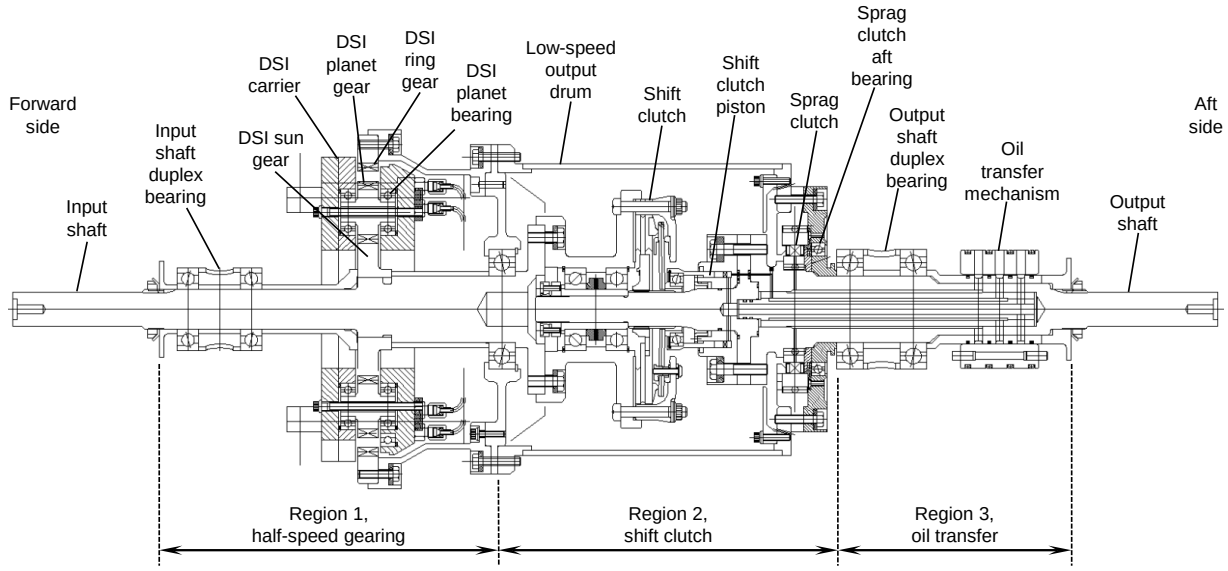

(a) Cross-sectional view.

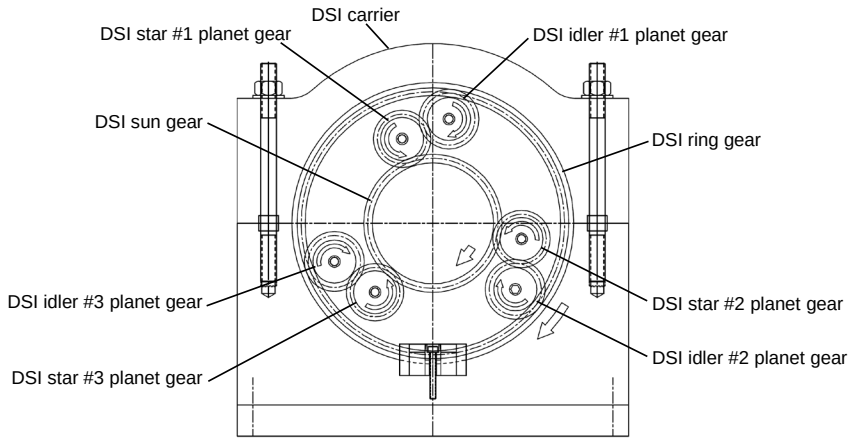

(b) Front view of DSI planetary.

Figure 8.—Dual star-idler (DSI) planetary transmission configuration.

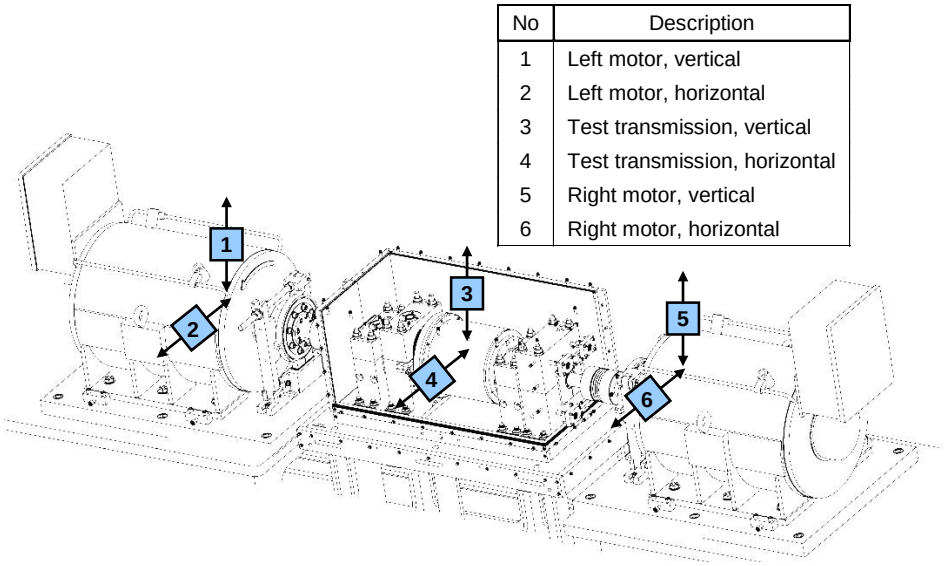

Figure 9.—Facility accelerometers.

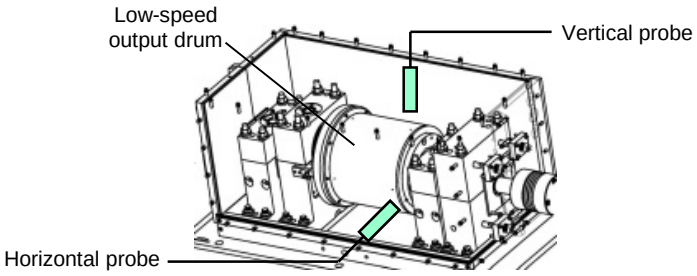

Figure 10.—Low-speed output drum proximity probes.

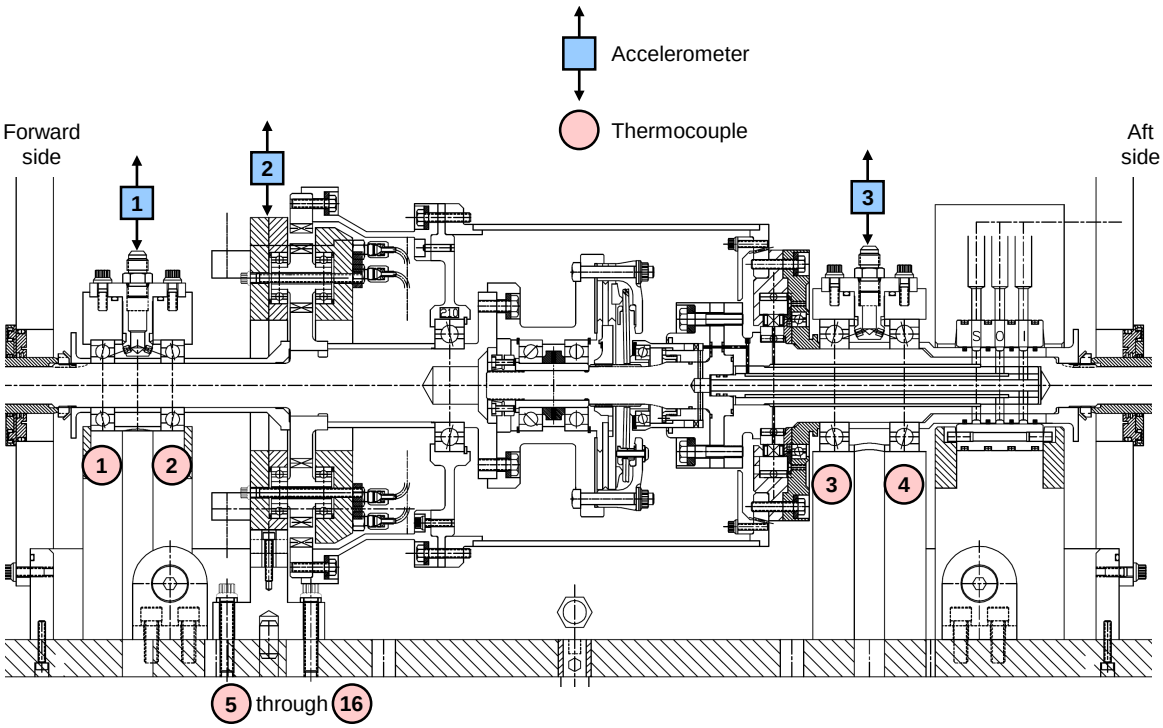

Acc No	Description
1	Input shaft duplex bearing housing
OCG:	
2	OCG cluster gear duplex bearing housing
DSI:	
2	DSI planetary carrier
3	Output shaft duplex bearing housing

TC No	Description
1	Input shaft duplex bearing, forward
2	Input shaft duplex bearing, aft
3	Output shaft duplex bearing, forward
4	Output shaft duplex bearing, aft
OCG:	
5	OCG cluster gear duplex bearing, forward
6	OCG cluster gear duplex bearing, aft
DSI:	
5	DSI, star #1 forward bearing
6	DSI, star #2 forward bearing
7	DSI, star #3 forward bearing
8	DSI, idler #1 forward bearing
9	DSI, idler #2 forward bearing
10	DSI, idler #3 forward bearing
11	DSI, star #1 aft bearing
12	DSI, star #2 aft bearing
13	DSI, star #3 aft bearing
14	DSI, idler #1 aft bearing
15	DSI, idler #2 aft bearing
16	DSI, idler #3 aft bearing

Figure 11.—Thermocouple and high-frequency accelerometer instrumentation.

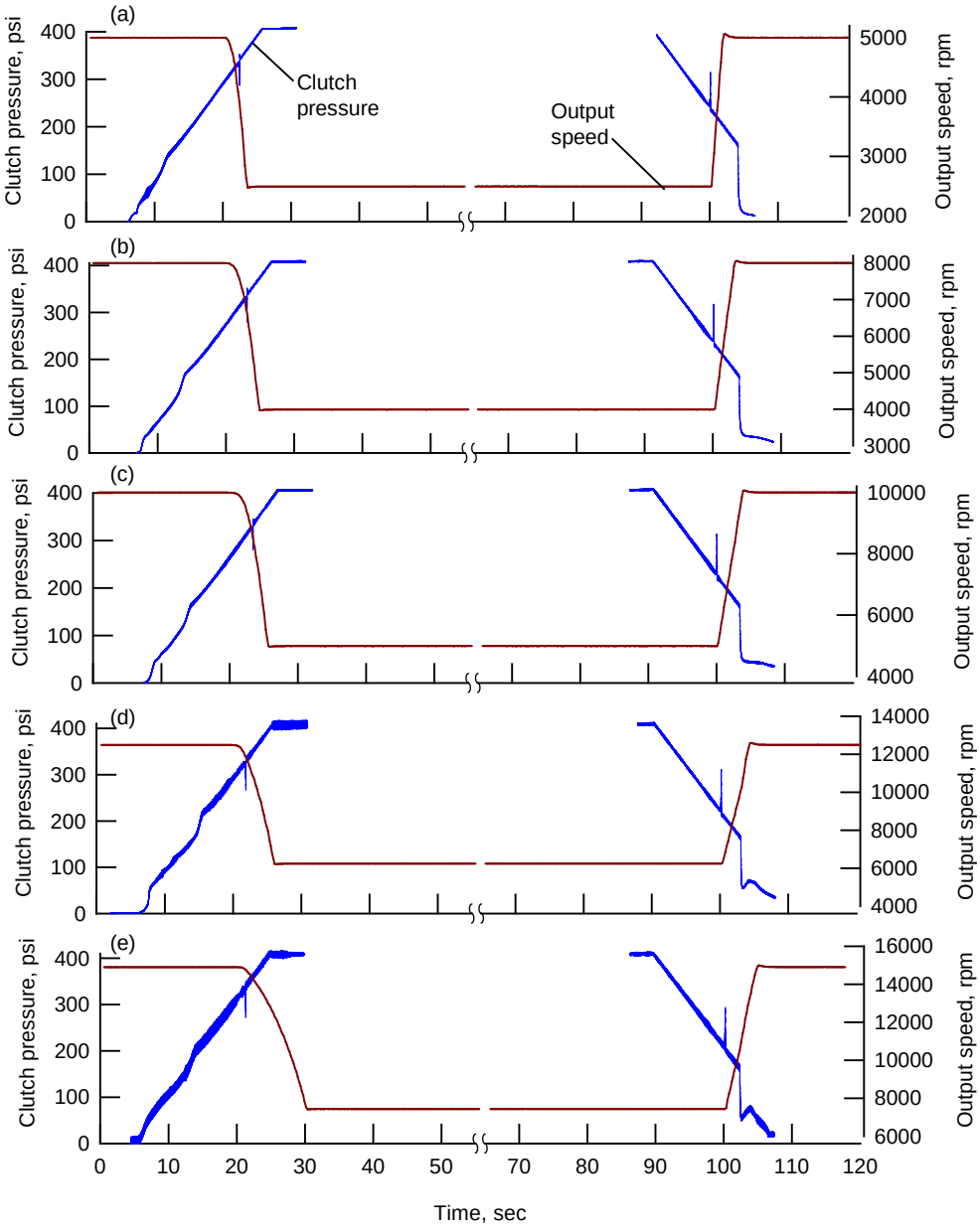

Figure 12.—Transmission output speed and clutch pressure for OCG shift tests. (a) 5,000 rpm input speed. (b) 8,000 rpm input speed. (c) 10,000 rpm input speed. (d) 12,500 rpm input speed. (e) 15,000 rpm input speed.

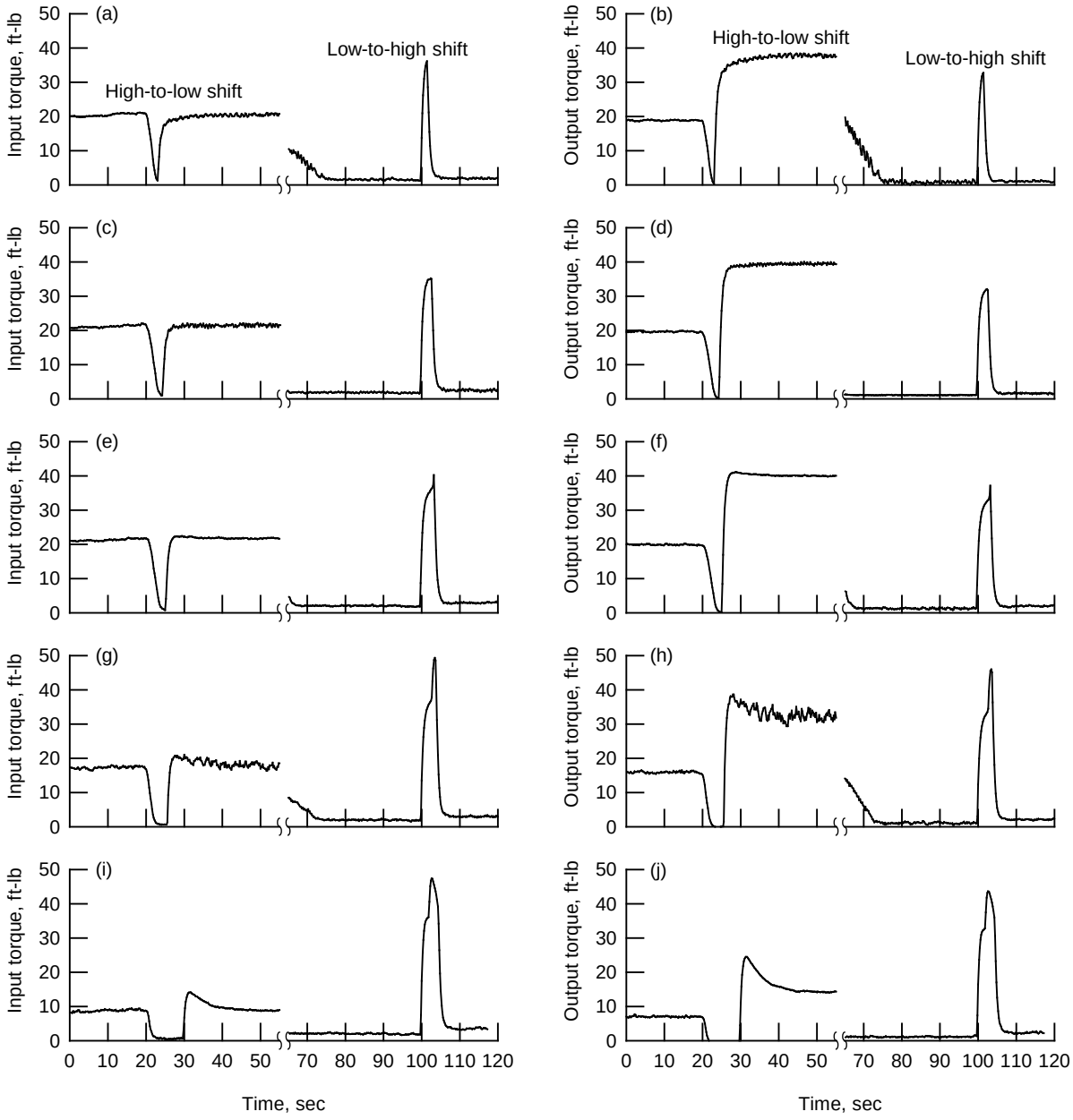

Figure 13.—Transmission input and output torques for OCG shift tests. (a) and (b) 5,000 rpm input speed. (c) and (d) 8,000 rpm input speed. e), f) 10,000 rpm input speed. (g) and (h) 12,500 rpm input speed. (i) and (j) 15,000 rpm input speed.

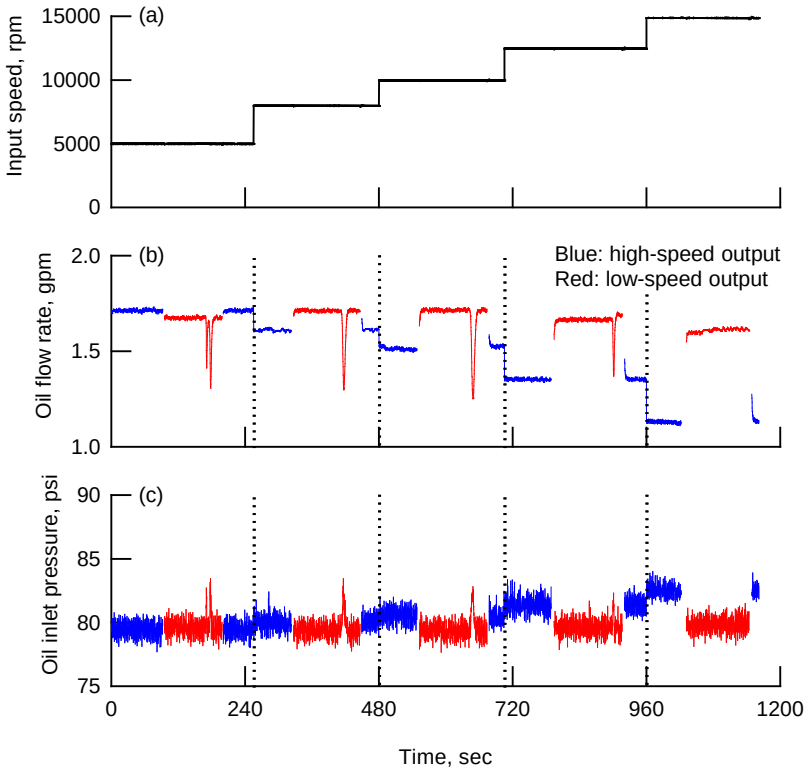

Figure 14.—Transmission lubrication characteristics for OCG shift tests.

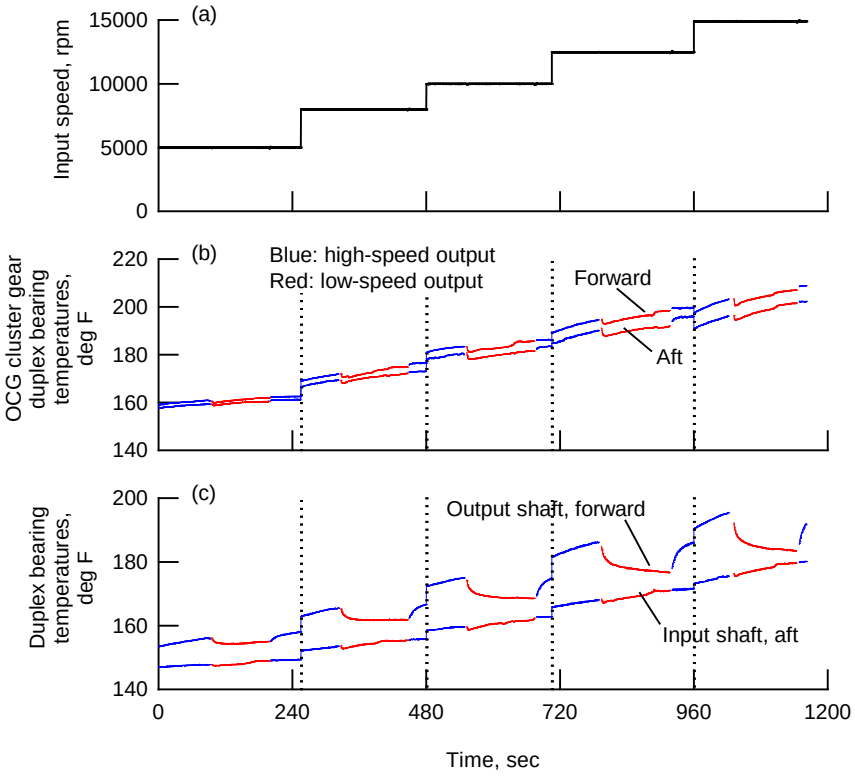

Figure 15.—Transmission temperatures for OCG shift tests.

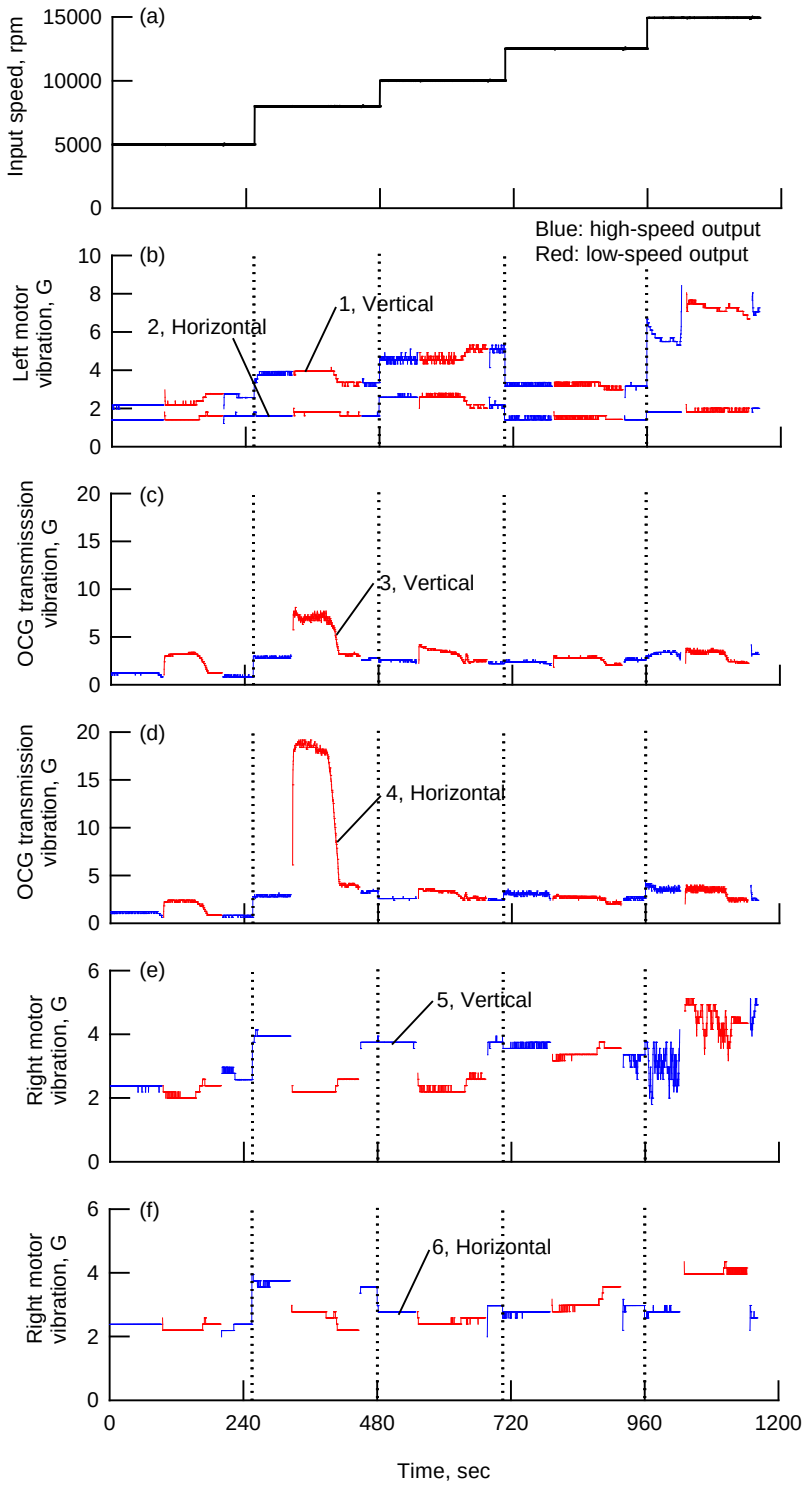

Figure 16.—Facility vibrations for OCG shift tests.

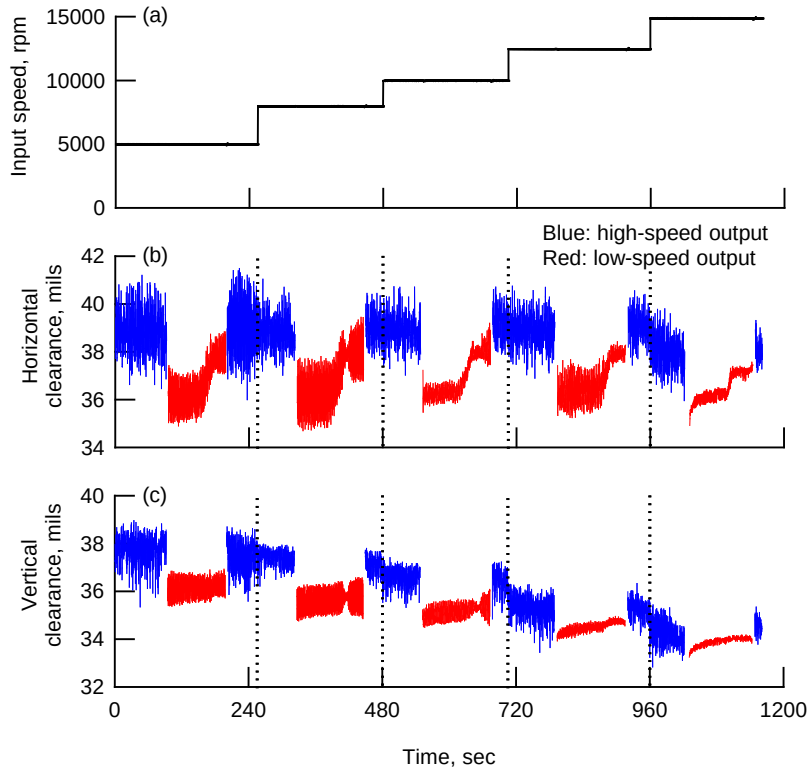

Figure 17.—Low-speed output shaft drum clearance from proximity probes for OCG shift tests.

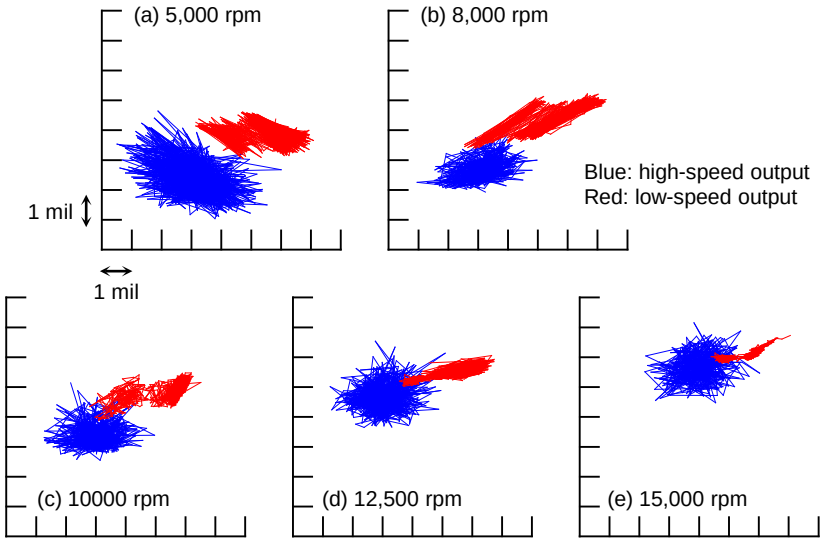

Figure 18.—Low-speed output shaft drum orbit from proximity probes for OCG shift tests.

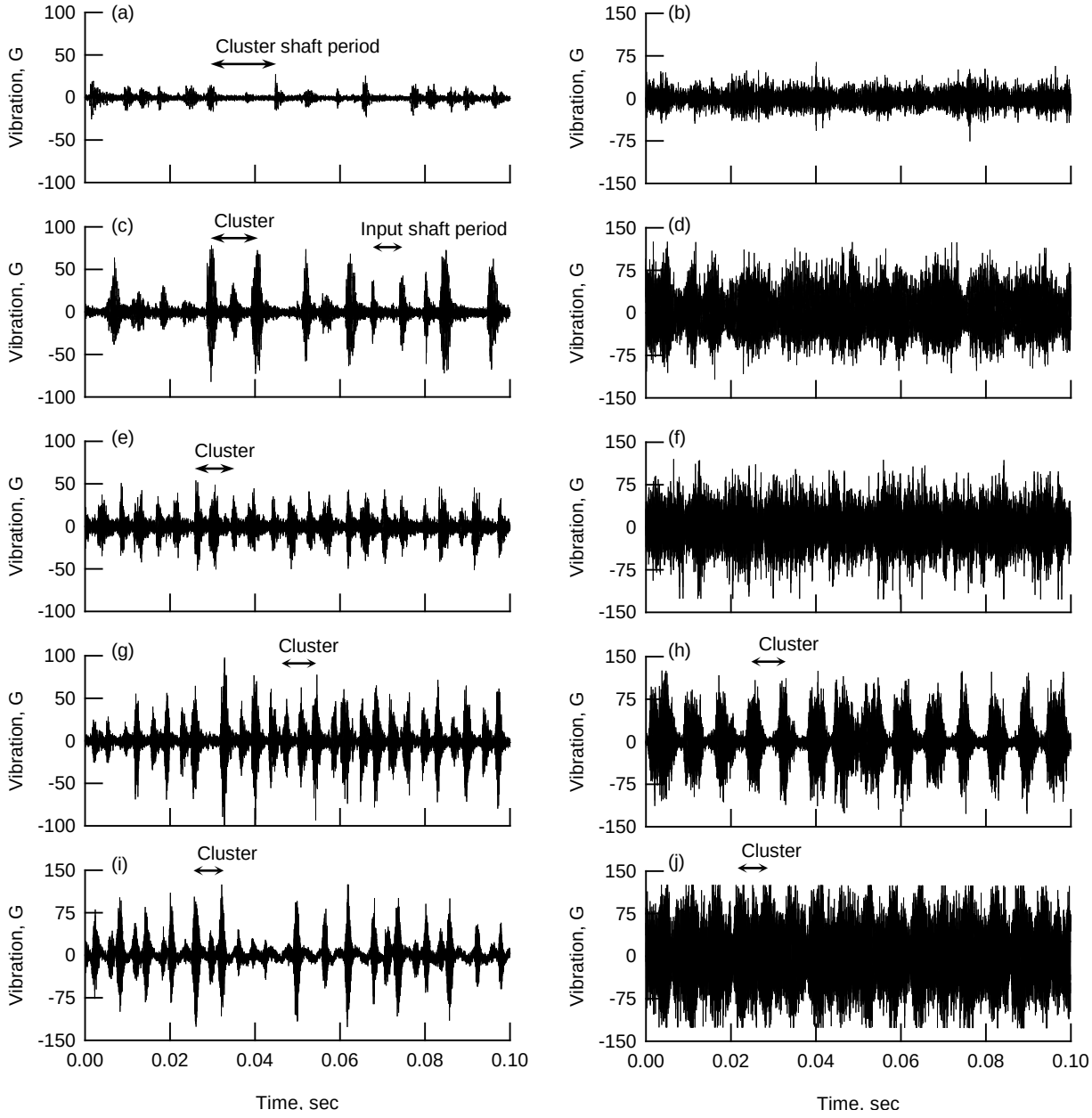

Figure 19.—OCG cluster gear duplex bearing housing (accelerometer 2) vibration time traces for OCG high-to-low speed shift tests. (a) 5,000 rpm input speed, 18.9 ft-lb output torque, before shift. (b) 5,000 rpm input speed, 37.8 ft-lb output torque, after shift. (c) 8,000 rpm input speed, 19.6 ft-lb output torque, before shift. (d) 8,000 rpm input speed, 39.4 ft-lb output torque, after shift. (e) 10,000 rpm input speed, 19.9 ft-lb output torque, before shift. (f) 10,000 rpm input speed, 40.1 ft-lb output torque, after shift. (g) 12,500 rpm input speed, 15.9 ft-lb output torque, before shift. (h) 12,500 rpm input speed, 32.5 ft-lb output torque, after shift. (i) 15,000 rpm input speed, 6.9 ft-lb output torque, before shift. (j) 15,000 rpm input speed, 14.1 ft-lb output torque, after shift.

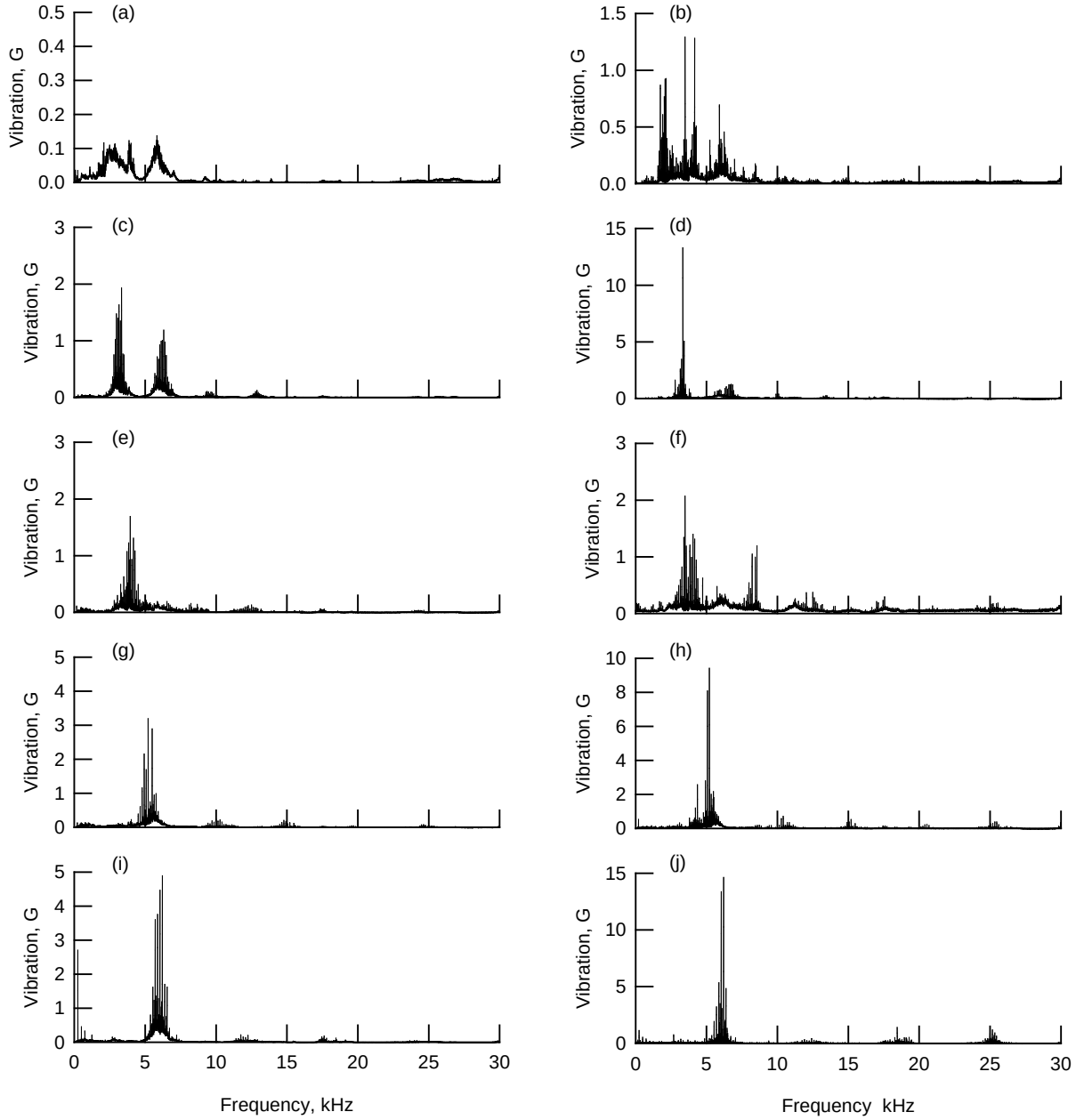

Figure 20.—OCG cluster gear duplex bearing housing (accelerometer 2) vibration spectra for OCG high-to-low speed shift tests. (a) 5,000 rpm input speed, 18.9 ft-lb output torque, before shift. (b) 5,000 rpm input speed, 37.8 ft-lb output torque, after shift. (c) 8,000 rpm input speed, 19.6 ft-lb output torque, before shift. (d) 8,000 rpm input speed, 39.4 ft-lb output torque, after shift. (e) 10,000 rpm input speed, 19.9 ft-lb output torque, before shift. (f) 10,000 rpm input speed, 40.1 ft-lb output torque, after shift. (g) 12,500 rpm input speed, 15.9 ft-lb output torque, before shift. (h) 12,500 rpm input speed, 32.5 ft-lb output torque, after shift. (i) 15,000 rpm input speed, 6.9 ft-lb output torque, before shift. (j) 15,000 rpm input speed, 14.1 ft-lb output torque, after shift.

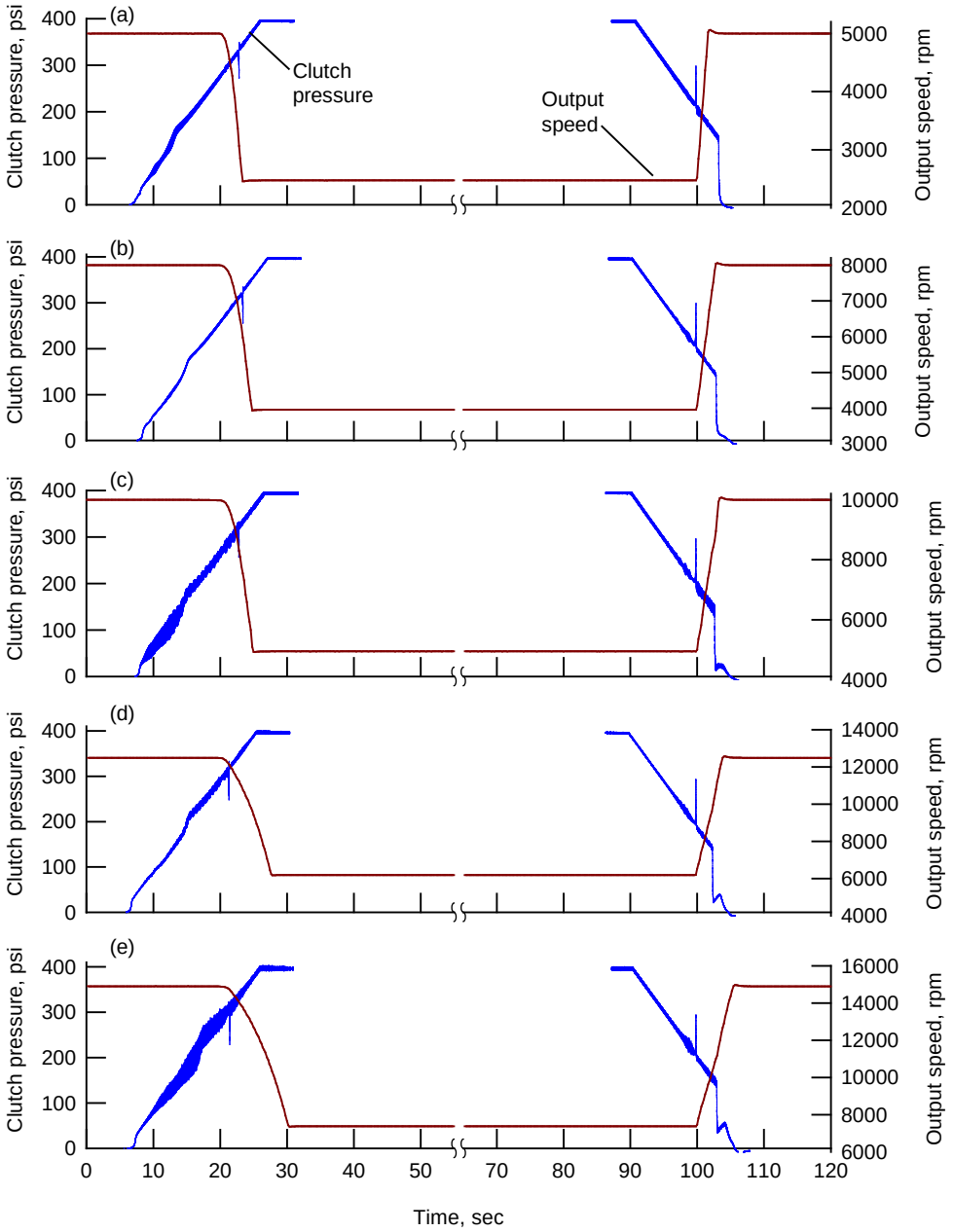

Figure 21.—Transmission output speed and clutch pressure for DSI shift tests. (a) 5,000 rpm input speed. (b) 8,000 rpm input speed. (c) 10,000 rpm input speed. (d) 12,500 rpm input speed. (e) 15,000 rpm input speed.

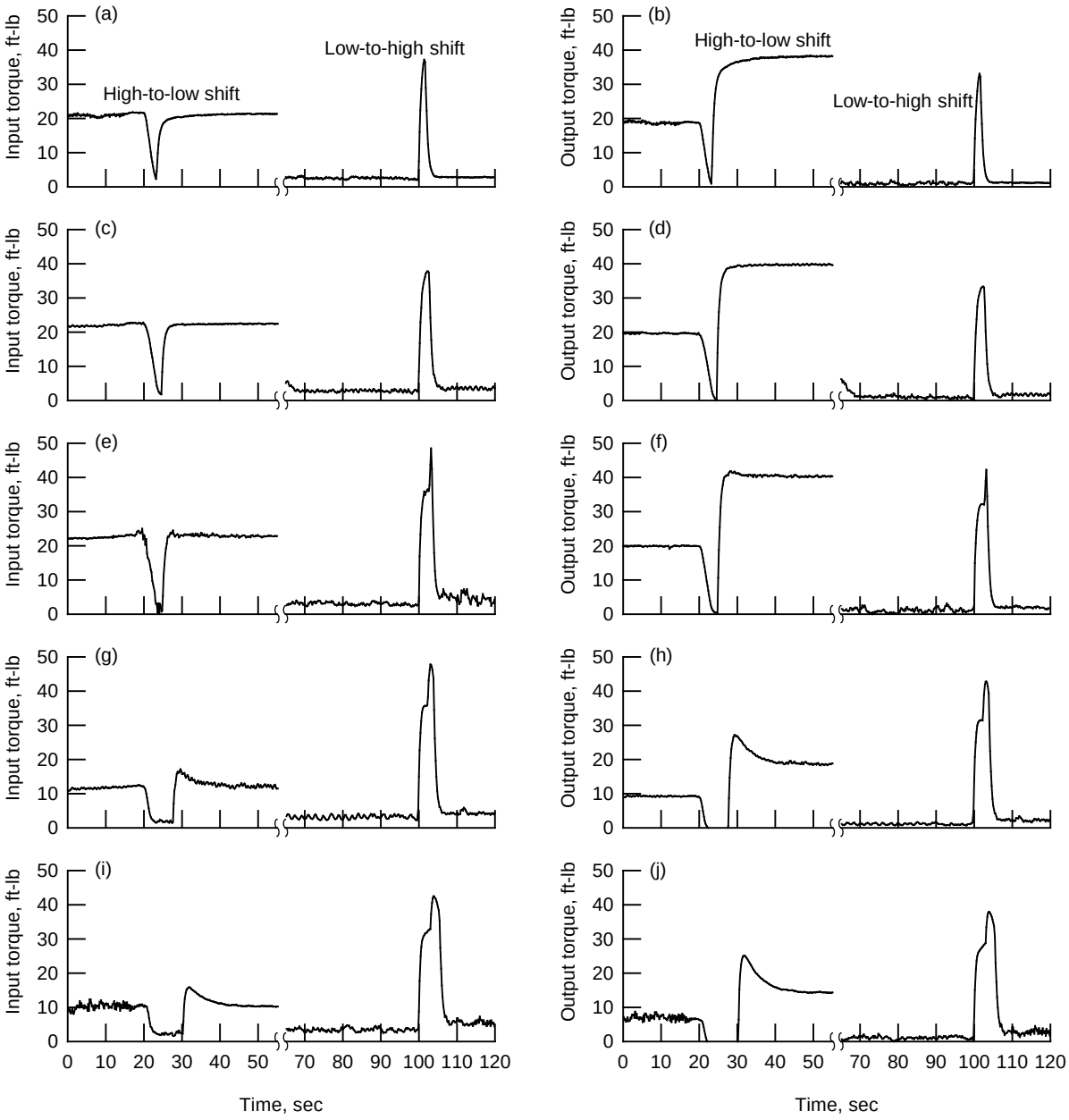

Figure 22.—Transmission input and output torque for DSI shift tests. (a) and (b) 5,000 rpm input speed. (c) and (d) 8,000 rpm input speed. (e) and (f) 10,000 rpm input speed. (g) and (h) 12,500 rpm input speed. (i) and (j) 15,000 rpm input speed.

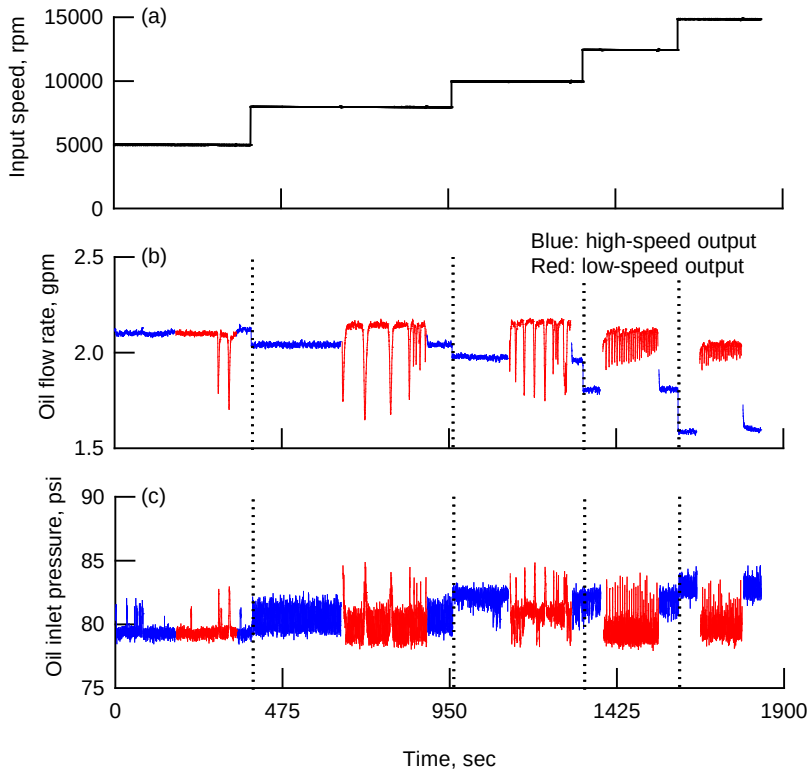

Figure 23.—Transmission lubrication characteristics for DSI shift tests.

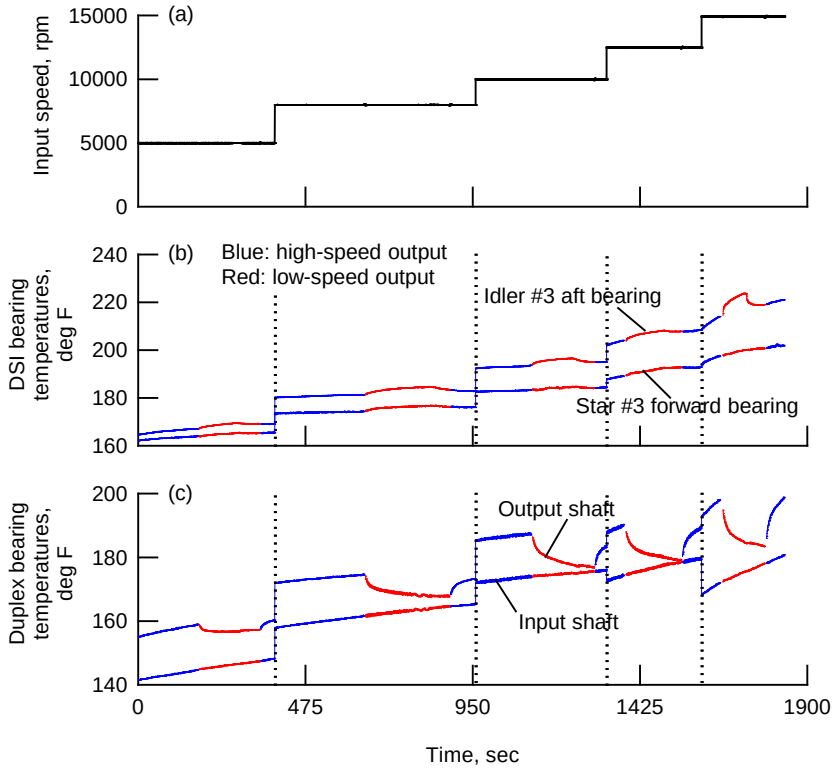

Figure 24.—Transmission temperatures for DSI shift tests.

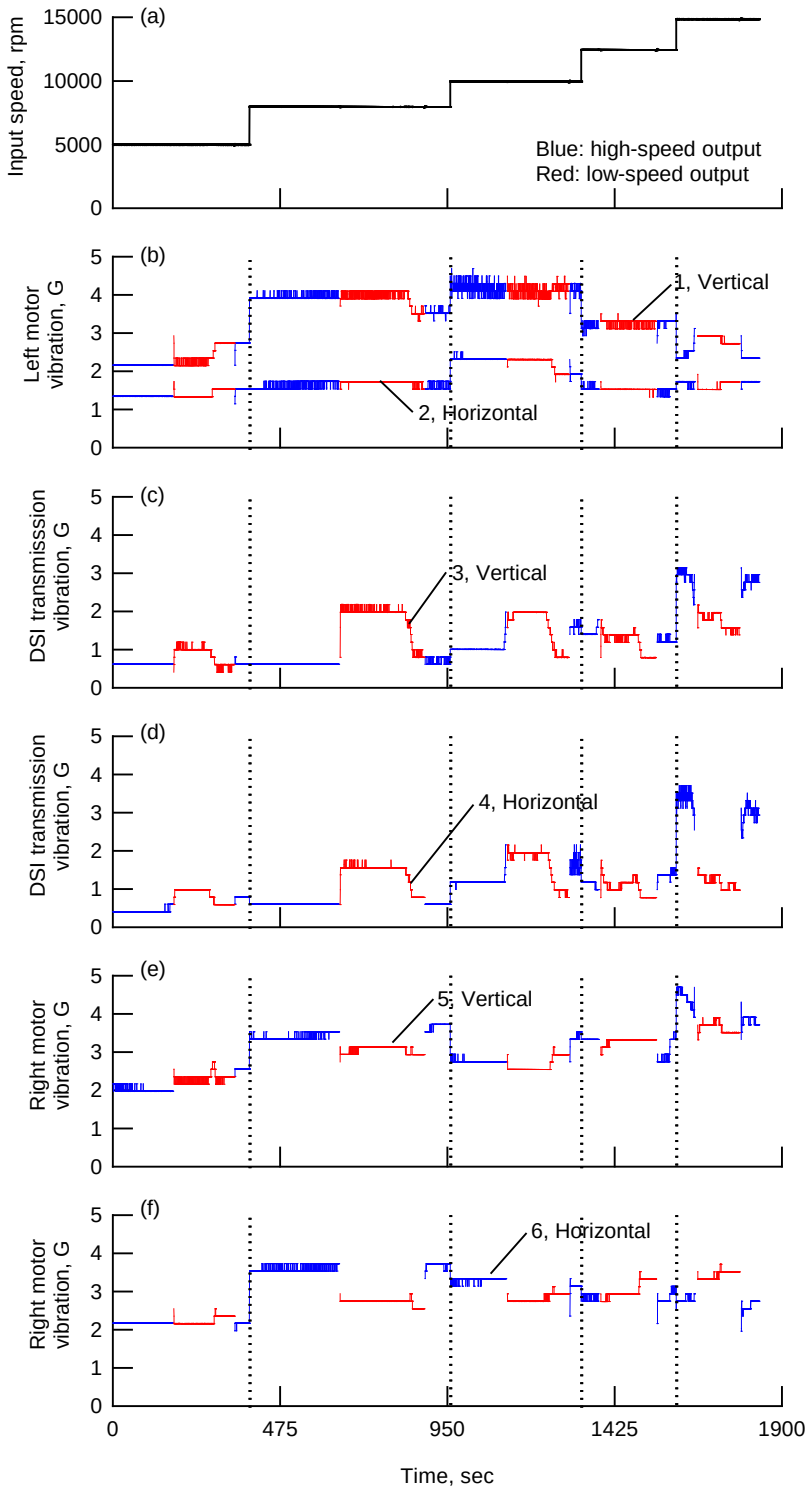

Figure 25.—Facility vibrations for DSI shift tests.

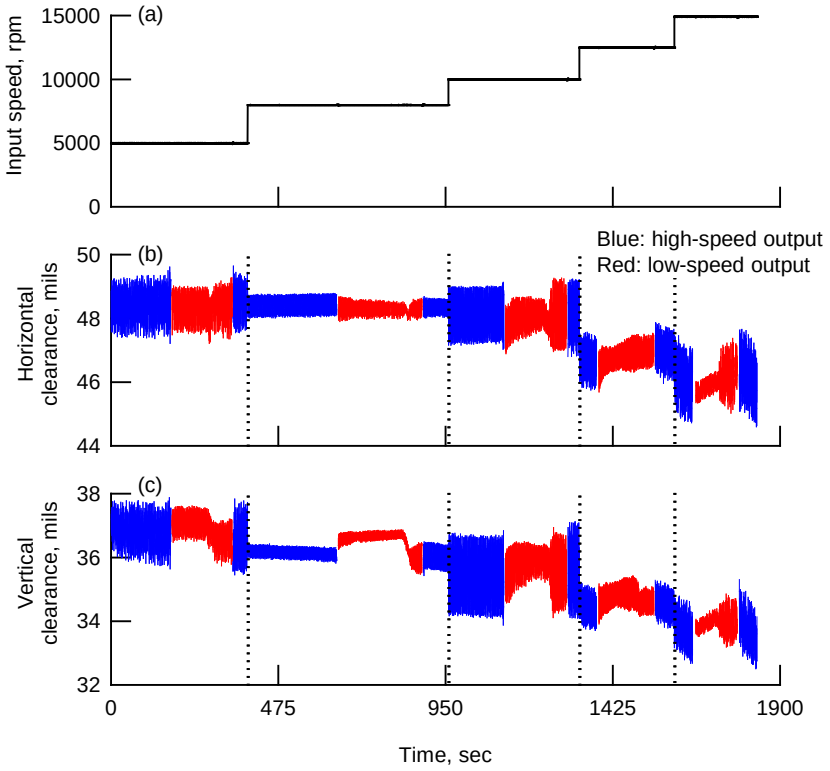

Figure 26.—Low-speed output shaft drum clearance from proximity probes for DSI shift tests.

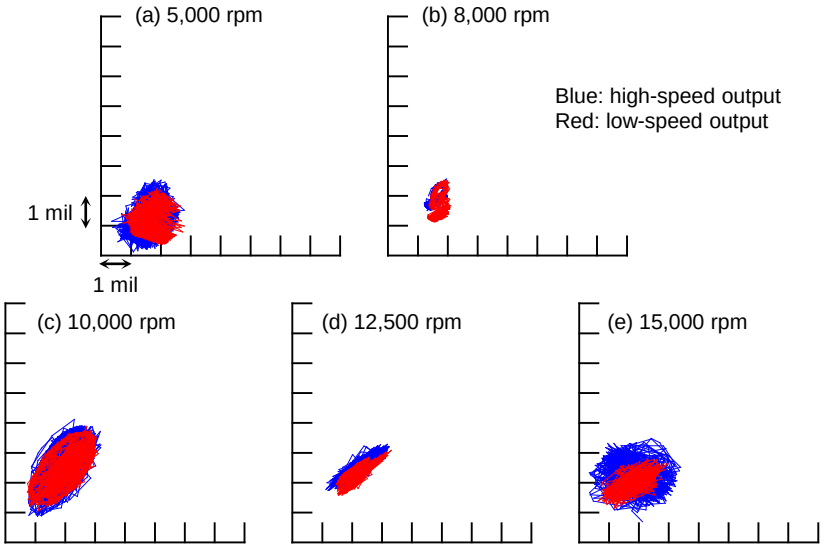

Figure 27.—Low-speed output shaft drum orbit from proximity probes for DSI shift tests.

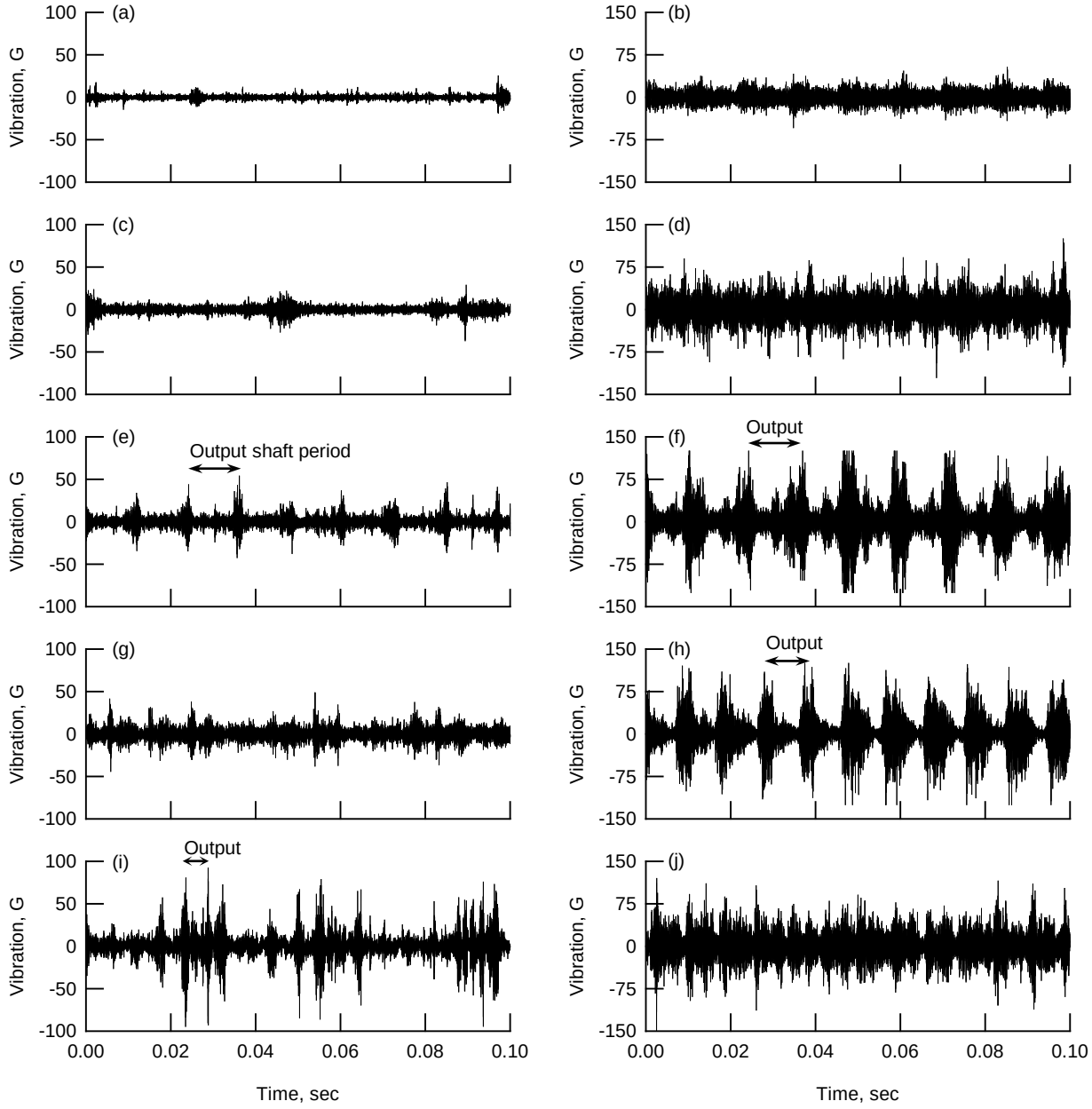

Figure 28.—DSI planetary carrier housing (accelerometer 2) vibration time traces for DSI high-to-low speed shift tests. (a) 5,000 rpm input speed, 19.1 ft-lb output torque, before shift. (b) 5,000 rpm input speed, 38.2 ft-lb output torque, after shift. (c) 8,000 rpm input speed, 19.7 ft-lb output torque, before shift. (d) 8,000 rpm input speed, 39.8 ft-lb output torque, after shift. (e) 10,000 rpm input speed, 20.0 ft-lb output torque, before shift. (f) 10,000 rpm input speed, 40.3 ft-lb output torque, after shift. (g) 12,500 rpm input speed, 9.2 ft-lb output torque, before shift. (h) 12,500 rpm input speed, 18.7 ft-lb output torque, after shift. (i) 15,000 rpm input speed, 7.0 ft-lb output torque, before shift. (j) 15,000 rpm input speed, 14.3 ft-lb output torque, after shift.

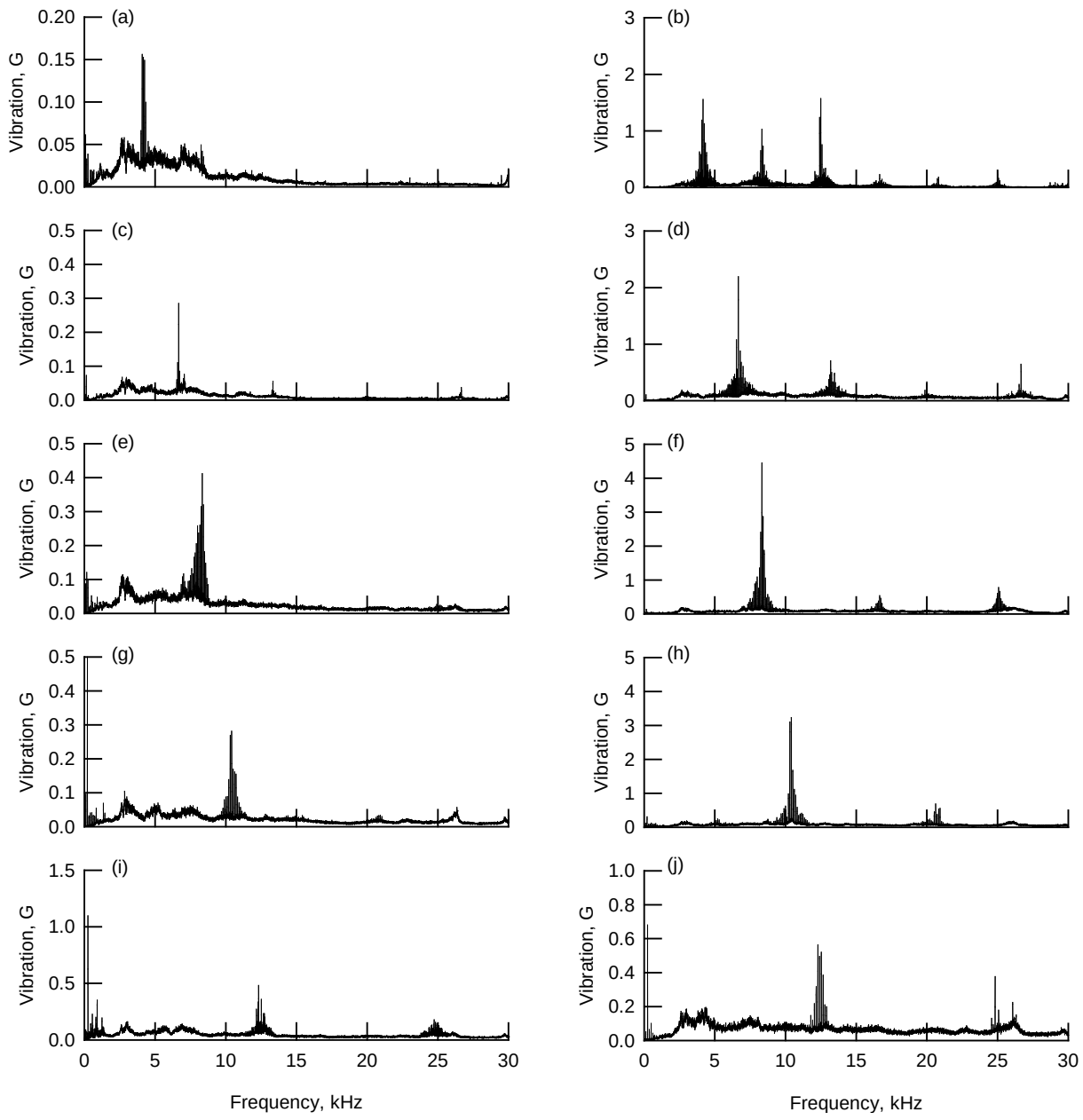

Figure 29.—DSI planetary carrier housing (accelerometer 2) vibration spectra for DSI high-to-low speed shift tests. (a) 5,000 rpm input speed, 19.1 ft-lb output torque, before shift. (b) 5,000 rpm input speed, 38.2 ft-lb output torque, after shift. (c) 8,000 rpm input speed, 19.7 ft-lb output torque, before shift. (d) 8,000 rpm input speed, 39.8 ft-lb output torque, after shift. (e) 10,000 rpm input speed, 20.0 ft-lb output torque, before shift. (f) 10,000 rpm input speed, 40.3 ft-lb output torque, after shift. (g) 12,500 rpm input speed, 9.2 ft-lb output torque, before shift. (h) 12,500 rpm input speed, 18.7 ft-lb output torque, after shift. (i) 15,000 rpm input speed, 7.0 ft-lb output torque, before shift. (j) 15,000 rpm input speed, 14.3 ft-lb output torque, after shift.

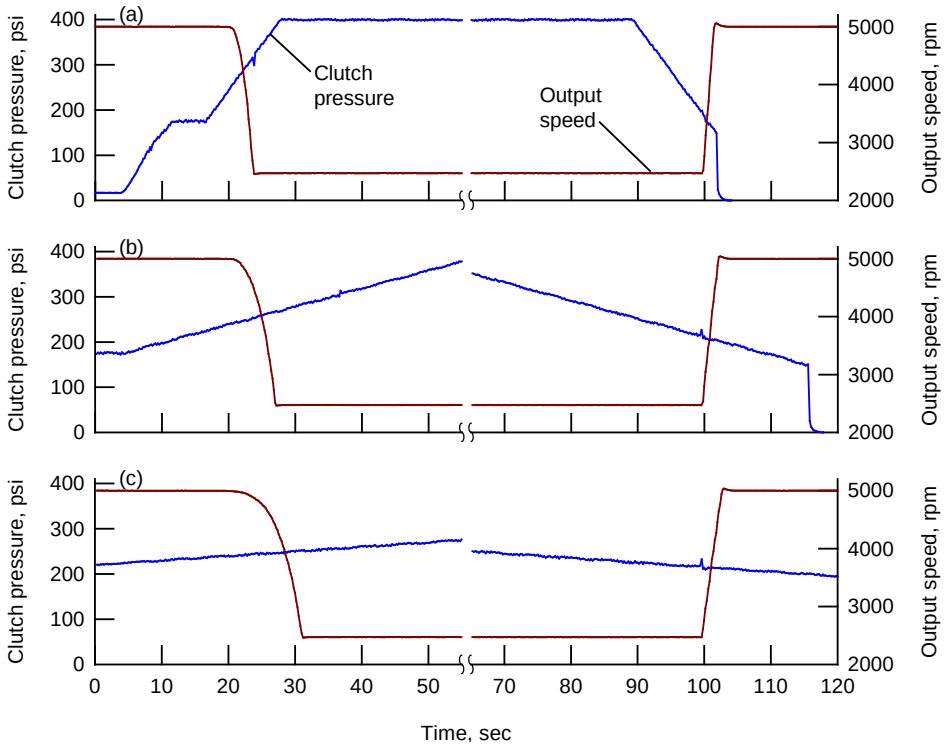

Figure 30.—Transmission output speed and clutch pressure for DSI power control shift tests. (a) 20 psi/sec clutch pressure ramp rate. (b) 4 psi/sec clutch pressure ramp rate. (c) 1 psi/sec clutch pressure ramp rate.

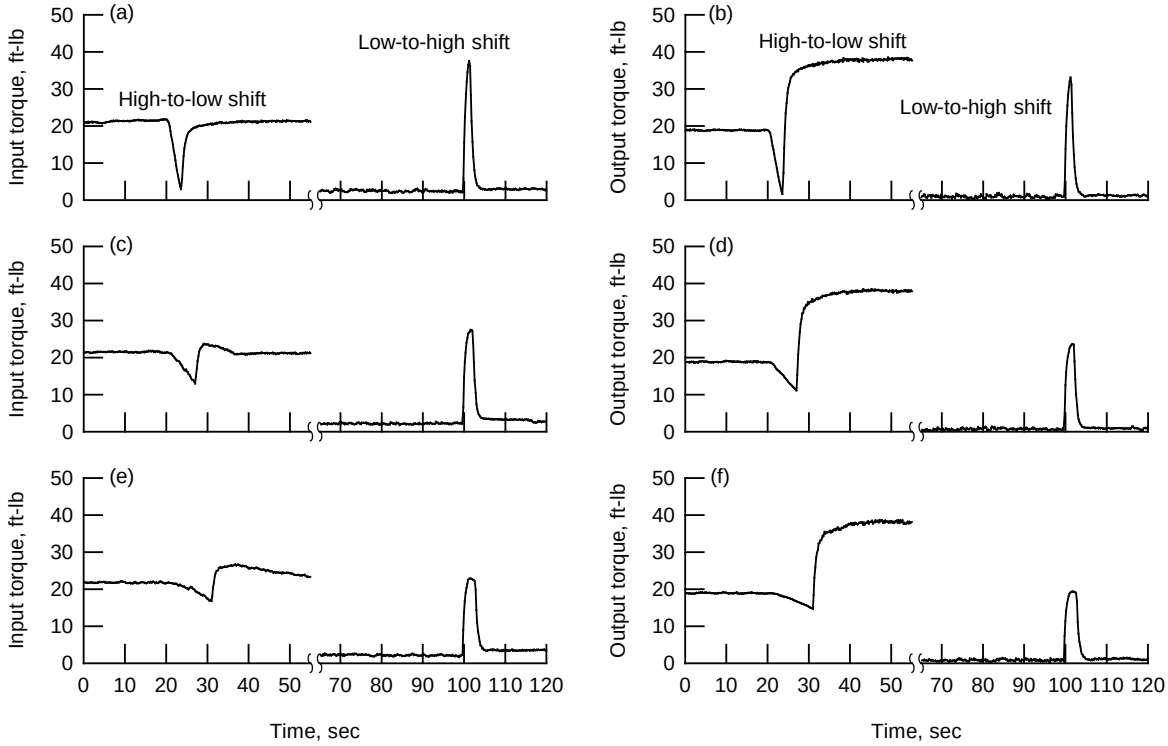

Figure 31.—Transmission input and output torque for DSI power control shift tests. (a) and (b) 20 psi/sec clutch pressure ramp rate. (c) and (d) 4 psi/sec clutch pressure ramp rate. (e) and (f) 1 psi/sec clutch pressure ramp rate.

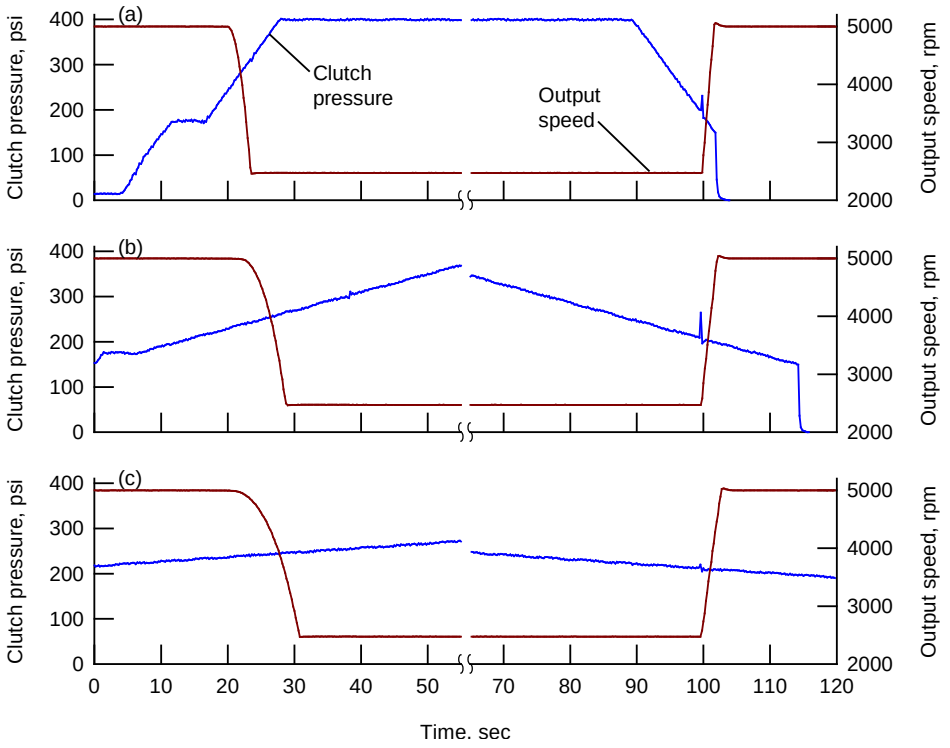

Figure 32.—Transmission output speed and clutch pressure for DSI torque control shift tests. (a) 20 psi/sec clutch pressure ramp rate. (b) 4 psi/sec clutch pressure ramp rate. (c) 1 psi/sec clutch pressure ramp rate.

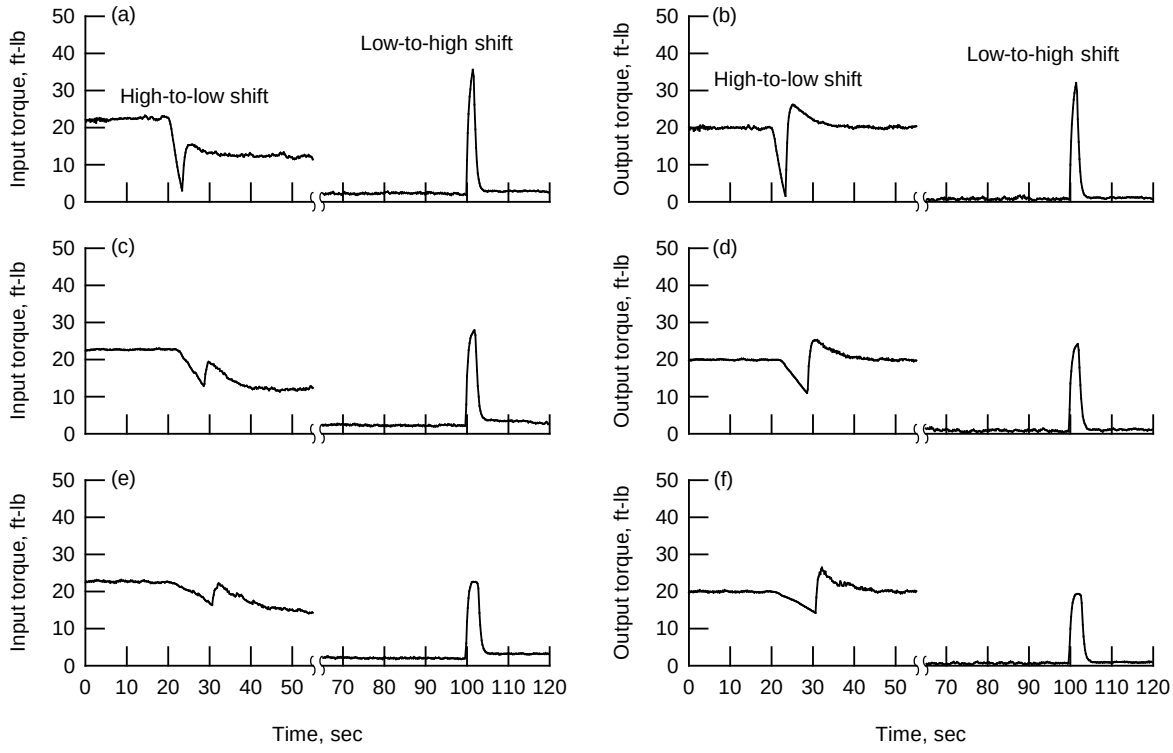

Figure 33.—Transmission input and output torque for DSI torque control shift tests. (a) and (b) 20 psi/sec clutch pressure ramp rate. (c) and (d) 4 psi/sec clutch pressure ramp rate. (e) and (f) 1 psi/sec clutch pressure ramp rate.

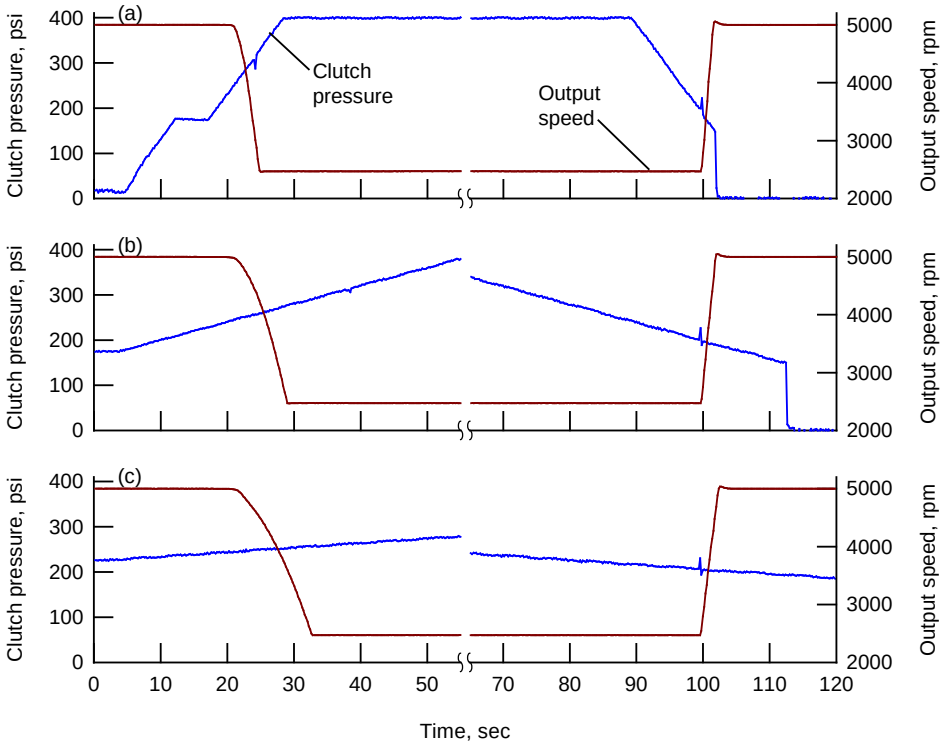

Figure 34.—Transmission output speed and clutch pressure for DSI manual control shift tests. (a) 20 psi/sec clutch pressure ramp rate. (b) 4 psi/sec clutch pressure ramp rate. (c) 1 psi/sec clutch pressure ramp rate.

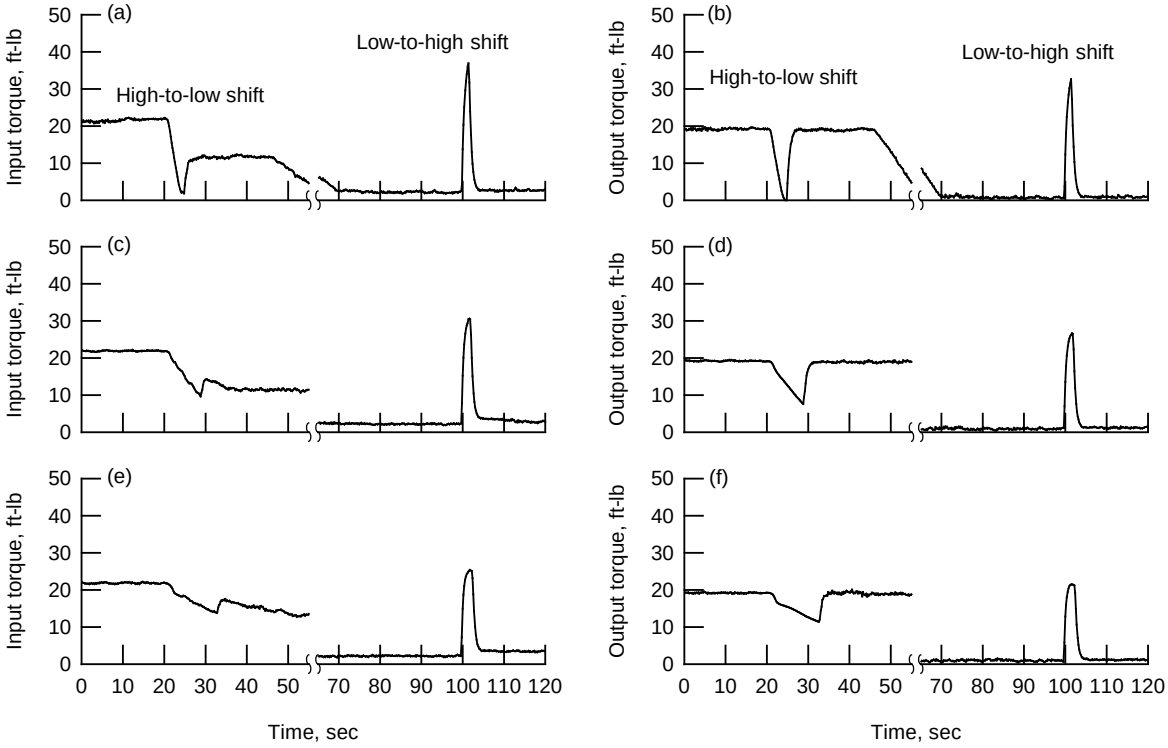

Figure 35.—Transmission input and output torque for DSI manual control shift tests. (a) and (b) 20 psi/sec clutch pressure ramp rate. (c) and (d) 4 psi/sec clutch pressure ramp rate. (e) and (f) 1 psi/sec clutch pressure ramp rate.

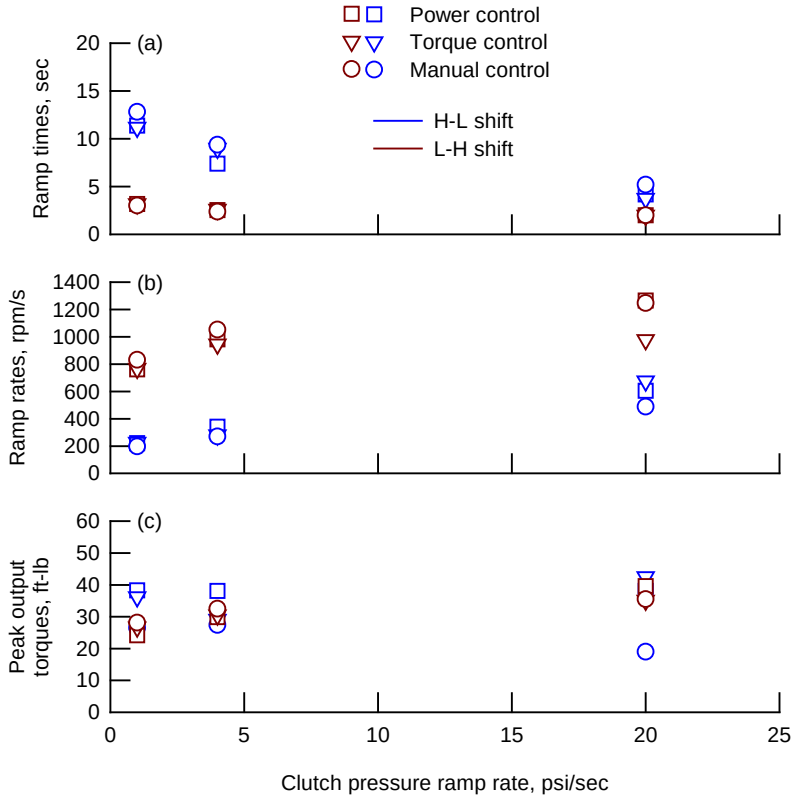

Figure 36.—Shift ramp times, rates, and peak output torque for DSI shift tests.

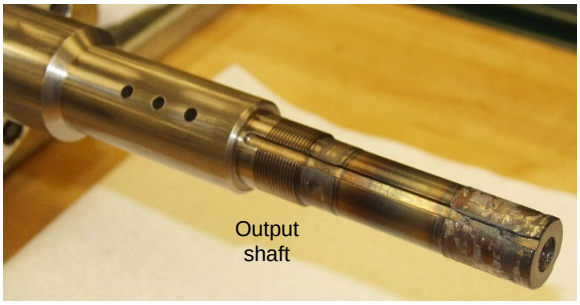

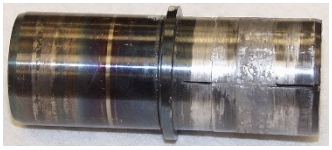

Sleeve

Figure 37.—Output shaft coupling failure.

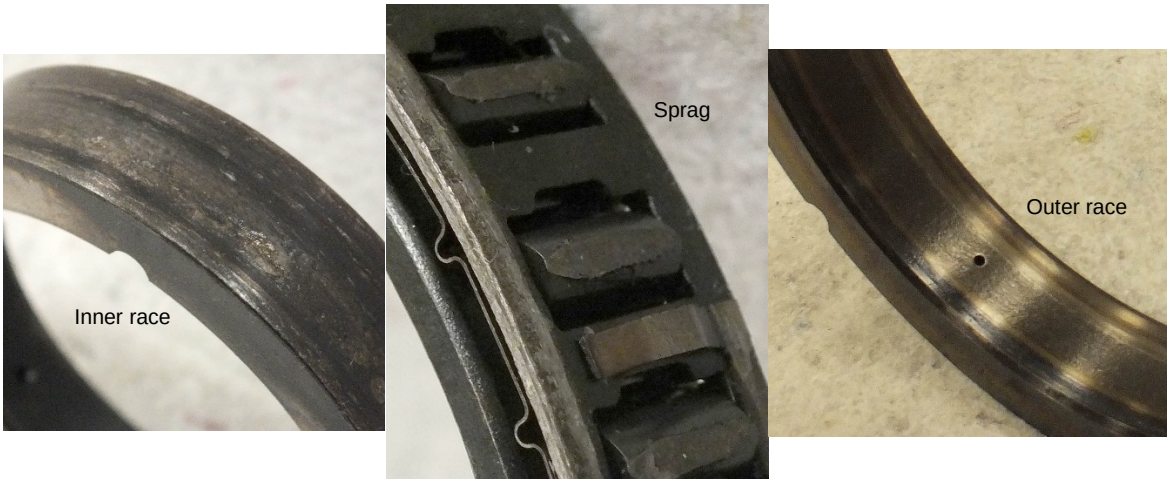

Figure 38.—Sprag clutch failure.

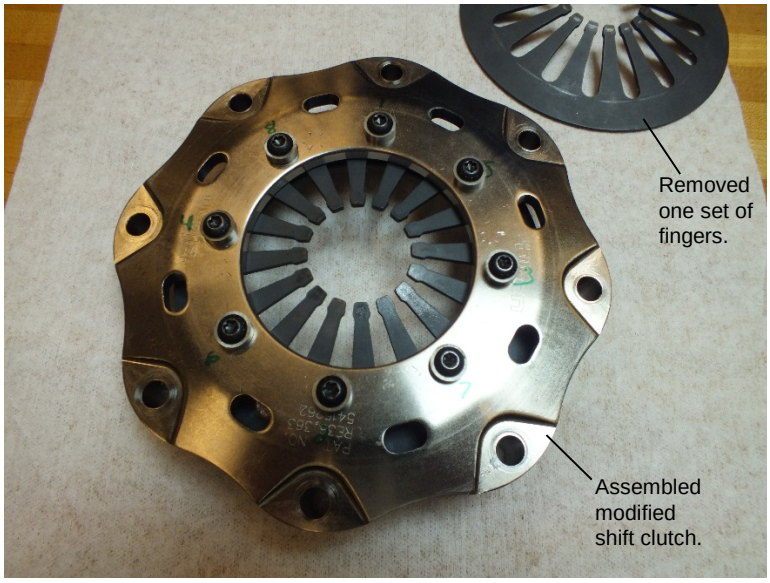

Figure 39.—Modified shift clutch.

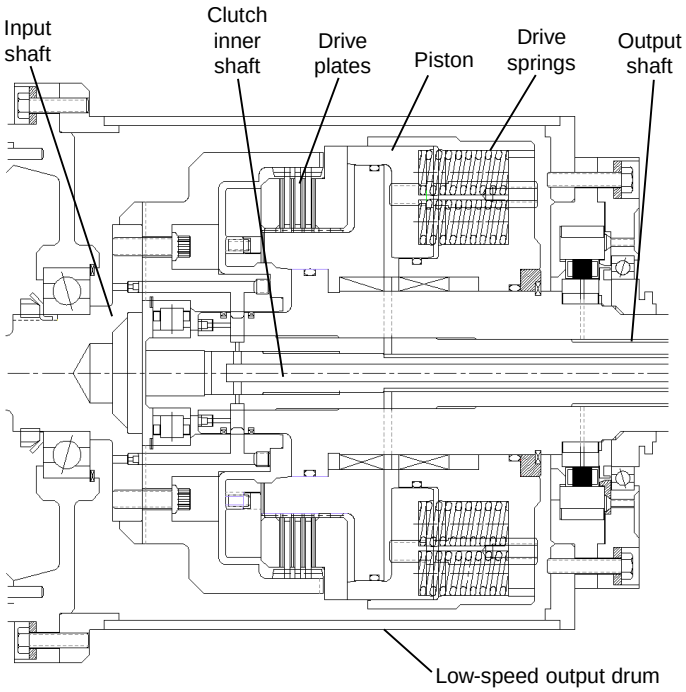

Figure 40.—Wet shift clutch.

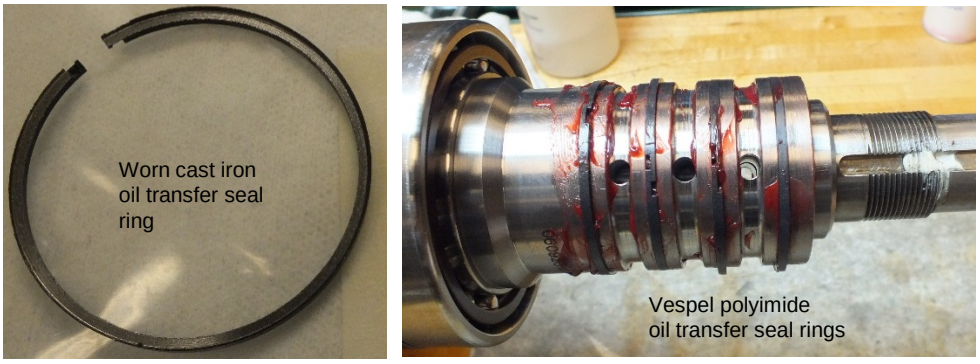

Figure 41.—Oil transfer seal rings.